



universität
wien

MAGISTERARBEIT

Titel der Magisterarbeit

Geophysical, geomorphologic and geological
investigations along the Lasse- Segment of the
Vienna Basin Transfer Fault System (VBTF)

Verfasser

Andreas Beidinger, Bakk. rer. nat.

Angestrebter akademischer Grad

Magister der Naturwissenschaften (Mag. rer. nat.)

Wien, 04.03. 2009

Studienkennzahl lt. Studienblatt: A 066 815

Studienrichtung lt. Studienblatt: Magisterstudium Erdwissenschaften

Betreuer: Univ. Prof. Mag. Dr. Bernhard Grasemann
Dr. Kurt Decker

Table of contents

1. Acknowledgements
2. Introduction
3. Seismic mapping and kinematics of the Lassee segment of the active Vienna Basin transfer fault system.
 - 3.1. Introduction
 - 3.2. Methodology
 - 3.3. Results and Interpretation
 - 3.3.1. Fault mapping
 - 3.3.2. Growth strata
 - 3.3.3. Geomorphology and Pleistocene basin evolution at the Lassee fault segment
 - 3.4. Discussion
 - 3.4.1. The Lassee Segment in a regional context
 - 3.4.2. The significance of normal fault branch faults (Markgrafneusiedl fault) for fault segmentation
 - 3.5. Conclusions
4. The Lassee Segment of the Vienna Basin Fault System as a potential source of the earthquake of *Carnuntum* in the 4th century A.D.
 - 4.1. Introduction
 - 4.2. Geological Background
 - 4.3. Methodology
 - 4.4. Results and Interpretation
 - 4.4.1. Tectonic Geomorphology
 - 4.4.2. Georadar
 - 4.5. Discussion
 - 4.6. Conclusions
5. References

Appendix

- I. Abstract
- II. Abstract (in German)
- III. Curriculum vitae (in German)

1. Acknowledgements

I want to thank all the people who helped to accomplish this diploma thesis with their professional or personal support.

I would like to give thanks to Dr. Kurt Decker and Univ. Prof. Mag. Dr. Bernhard Grasemann for the mentoring of the diploma thesis. A special thank goes to Dr. Kurt Decker for giving me the opportunity to work on this very exciting topic, and for excellent supervision by providing professional support, patience and a lot of time for discussion.

I also want to thank Ao. Univ. Prof. Dipl.-Ing. Dr. Karl-Heinz Roch for enabling the GPR survey by providing the equipment and his professional support, as well as for the processing of GPR data.

Further I want to give thanks to Christian Astl and Philipp Strauss from OMV Austria for providing the data used for seismic interpretation.

My gratitude also goes to many colleagues and friends at the Department of Geodynamics and Sedimentology at the University of Vienna. I want to thank Monika Hölzel, Maria Hoprich, Iris Lenauer, Lukas Plan, Bernhard Salcher and András Zámolyi for the excellent working atmosphere and a lot of help during the last two years.

A special thank goes to Anton Tanzberger and Christoph Tuitz. Thanks for your friendship and the many indispensable scientific discussions since the beginning of our course of studies at the university.

Last and for sure not least I want to express my gratefulness to my whole family that made it possible for me to realize my studies. Thanks for your essential patience, encouragement, motivation and financial support during the whole time of my studies.

2. Introduction

The diploma thesis comprises the subject area of structural geology with emphasis on active tectonics. It includes the integration of data from geological, tectonic-geomorphologic and geophysical studies along a fault segment at the active Vienna Basin Fault System. The objective is the reconstruction of 3D geometries of faults, as well as of the youngest faulting history, along the Lassesee Segment. The segment is situated at the southern border of the Vienna Basin some 30 km E of Vienna.

The work was accomplished under the supervision of Dr. Kurt Decker und O. Univ. Prof. Mag. Dr. Bernhard Grasemann at the Department of Geodynamics and Sedimentology at the University of Vienna. The time period of investigations was from spring 2007 to winter 2008.

Studies can be divided into two subareas:

- A. Spatial fault mapping along the Lassesee Segment using 2D seismic lines and tectonic geomorphology
- B. Ground penetrating radar studies and tectonic geomorphology along the northwestern scarp of the Pleistocene Schlosshof terrace

ad. A:

Fault mapping uses 14 2D seismic lines covering the Pleistocene Lassesee Basin and adjacent terraces, which were provided by OMV Austria. The mapping was done by means of the seismic interpretation software *Seisvision* *GeoGraphix*. In order to obtain information on 3D geometries of subsurface faults, respectively on continuous activity during Quaternary times, the interpretation was supported by tectonic geomorphology and Pleistocene Basin analyses. Here the main focus was the interaction of tectonics and Pleistocene landscape evolution. For this purpose the results from seismic interpretation were integrated with a digital elevation model of Lower Austria and Quaternary thickness data using the software *ArcGis*. The interpretation was supplemented by using the 3D seismic block "Marchfeld" (by the courtesy

of OMV Austria), which barely covers the study region. By utilization of further 2D seismic data in the northern and southern continuation of the Lassee Segment additional information on the kinematics along the different segments could be obtained.

ad. B:

For the reconstruction of the youngest faulting history along the Lassee Segment, GPR studies were performed at the northwestern scarp of the Schlosshof terrace. These studies were supplemented by tectonic geomorphology. Tectonic geomorphology includes topographic analysis of valleys cutting down the scarps bordering the triangular shaped terrace and precision leveling of a selected hanging valley at the northwestern scarp of the Schlosshof terrace.

GPR data acquisition was conducted during spring 2007 in cooperation with the Vienna University of Technology (TU Vienna) under the supervision of Ao. Univ. Prof. Dipl.-Ing. Dr. Karl-Heinz Roch (Institute of Geodesy and Geophysics, TU Vienna). The GPR equipment was provided by the TU Vienna, whereas the processing of data was performed by Ao. Univ. Prof. Dipl.-Ing. Dr. Karl-Heinz Roch.

In the present manuscript the two following sub-topics are treated separately:

Chapter 3:

Seismic mapping and kinematics of the Lassee segment of the active Vienna Basin transfer fault system.

Chapter 4:

The Lassee Segment of the Vienna Basin Fault System as a potential source of the earthquake of Carnuntum in the 4th century A.D..

Both topics are presented in a format comprising a subdivision into the chapters introduction, methodology, results and interpretation, discussions and conclusions.

3. Seismic mapping and kinematics of the Lasse segment of the active Vienna Basin transfer fault system

3.1. Introduction

The Vienna Basin Fault System is a seismotectonically active sinistral strike-slip fault between the Eastern Alps, West Carpathians and the Pannonian basin. The NE-striking fault cuts the external parts of the Alpine-Carpathian thrust units delimiting a stable W block, which overlies European foreland, from a NE-ward moving unit E of the fault (Fig. 1). Sinistral strike-slip faulting is related to the NE-directed lateral escape of the crustal block E of the fault, which includes the easternmost parts of the Alps, the western Pannonian basin and parts of the West Carpathians (Gutdeutsch & Aric, 1988; “Styrian-West Carpathian Wedge”: Decker et al., 2005). Earthquake data highlight the NE-striking fault as a zone of moderate seismicity (Fig. 2). The largest historically and instrumentally recorded earthquakes reach $I_{\max} = 8 - 8.5$ corresponding to $M_{\max} = 5.2 - 5.7$ (Schwadorf, 1925; Dobra Vodá, 1906; ZAMG, 2008; ACORN, 2004; Fig. 2).

The fault system developed during the Miocene lateral extrusion of the central Eastern Alps towards the Pannonian region, which occurred between (E)NE-striking sinistral and (E)SE-striking trending dextral faults delimiting extruding crustal wedges to the N and S, respectively (Ratschbacher et al., 1991a, b; Linzer et al., 1997; 2002). Major extrusion-related wrench faults include the sinistral SEMP (Salzach-Ennstal-Mariazell-Puchberg) fault system and the dextral Peradriatic fault, which were mostly active during the Oligocene and Early Miocene (Urbanek et al., 2002; Glodny et al., 2008), and the Middle to Late Miocene faults of the sinistral Vienna Basin Fault System and the dextral Lavanttal fault (Fig. 1; Ratschbacher et al., 1991b; Decker, 1996). The formation of the Vienna Basin Fault System is dated by the onset of subsidence in the Vienna Basin, which opened as a pull-apart between two left stepping segments of the fault zone (Fig. 1; Royden, 1985, 1988; Wessely, 1988; Sauer et al., 1992; Fodor, 1995). The onset of pull-apart subsidence is well dated by growth strata. Syntectonic sedimentation started

with the deposition of the Aderklaa Conglomerate Member (Aderklaa Fm.) during the Badenian (c. 16.1 Ma; Kovac et al. 2004; Strauss et al. 2006) and continued up to the Upper Pannonian (c. 9-8 Ma; Rögl et al., 1993). Significant volumes of Pontian and Pliocene sediments are not known from the Vienna Basin (Rögl, 1996) suggesting that pull-apart subsidence terminated at about 9-8 Ma.

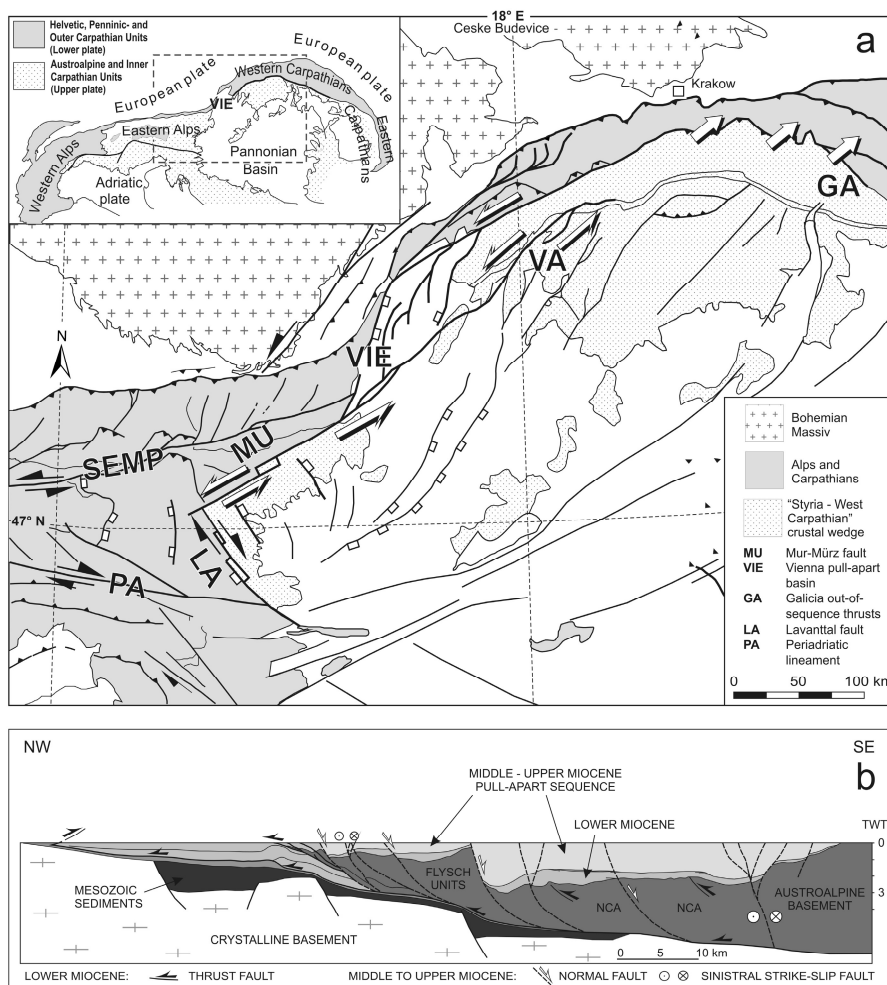


Fig. 1. (a) Tectonic map of the transition between Eastern Alps, West Carpathians and Pannonian Basin highlighting Oligocene and Miocene faults. The Mur-Mürz-Vienna Basin transfer fault system (MU, VIE) and its continuation into the Vah Valley (VA) formed during Middle to Upper Miocene NE-directed lateral extrusion of the Styrian-West Carpathian wedge. The Vienna pull-apart basin (VIE) developed between two left stepping segments of the fault. Other faults related to lateral extrusion are the Oligocene to Early Miocene Salzachtal-Ennstal-Mariazell-Puchberg fault (SEMP), the Periadriatic fault (PA) and the Middle to Upper Miocene Lavanttal fault (LA). (b) Geological cross section through the Vienna Basin and the adjacent Molasse foreland basin. Strike-slip and normal faults of the pull-apart basin root in the floor thrust of the Alpine thrust wedge forming a basal detachment at 5 – 6 s TWT (c. 10 km depth).

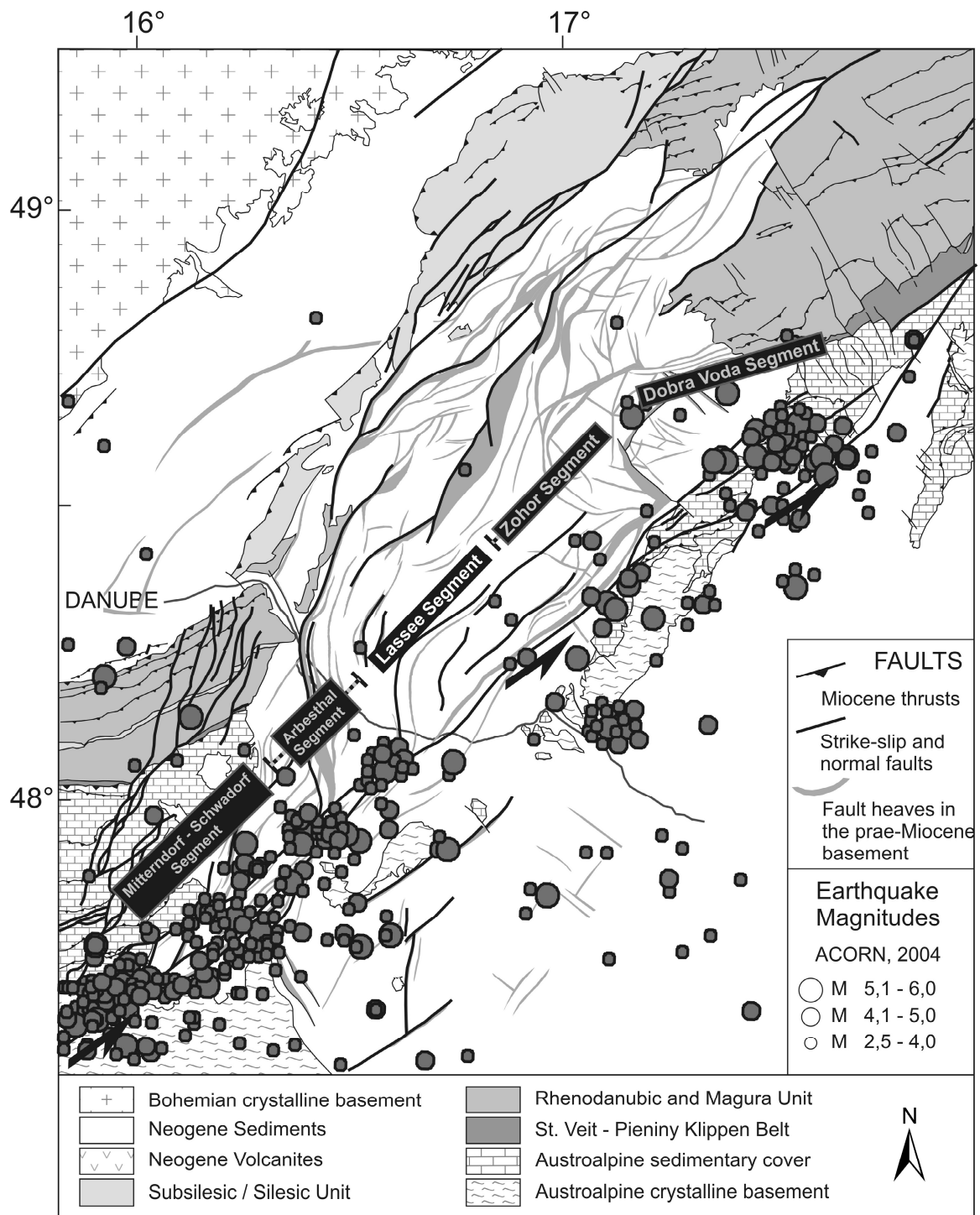


Fig. 2. Tectonic map of the Vienna Basin and distribution of seismicity at the Vienna Basin Transfer fault system. Fault heaves in pre-Miocene basement from Kröll & Wessely, 1993.

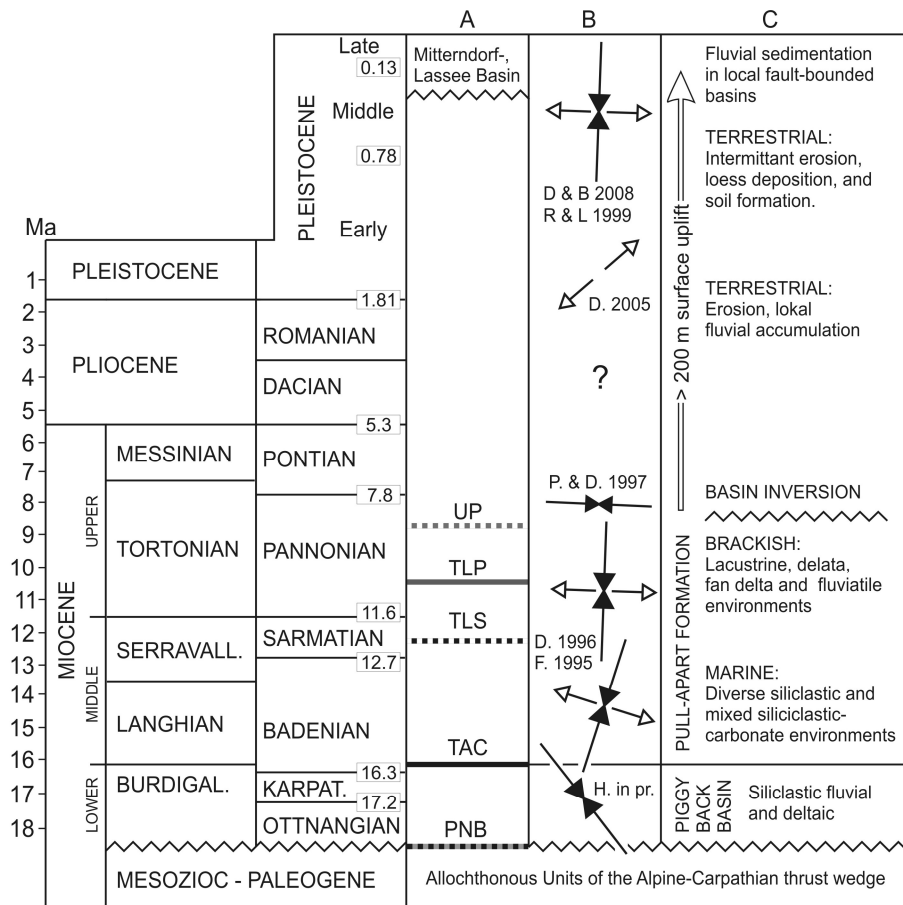


Fig. 3. Stratigraphy and evolution of the Vienna Basin from the Miocene to the present. Columns refer to standard chronostratigraphy (left, after Gradstein and Ogg, 2004) and correlated Central Paratethys stages used in this paper (Piller et al., 2004). Column A: Stratigraphic position of the mapped horizons PNB (Top Pre-Neogene Basement), TAC (Top Aderklaa Conglomerate Mbr.), TLS (Top Lower Sarmatian), TLP (Top Lower Pannonian) and UP (horizon in the Upper Pannonian). B: Tectonic events indicated by shortening / extension directions (from Fodor, 1995; Decker, 1996; Peresson & Decker, 1997; Decker et al., 2005; Reinecker & Lenhardt, 1999; Decker & Burmester, 2008; Hölzel et al., in press). C: Sedimentary evolution of the basin (Strauss et al., 2004; Salcher et al., submitted).

The Miocene basin formed as a thin skinned pull-apart with extension restricted to the upper crust above the floor thrust of the Alpine Carpathian thrust sheets, which form a basal detachment for strike-slip and extensional faulting (Fig. 1; Royden, 1988). Structural maps of the pull-apart basin highlight several large listric normal faults (Leopoldsdorf Fault, Steinberg Fault) with vertical offsets of up to 5.5 km connecting the two left-stepping strike slip faults (Kröll & Wessely, 1993; Wessely, 1988; Decker, 1996; Decker et al., 2005). These normal faults are located at the NW border of the basin resulting in an asymmetric basin shape with a growth strata wedge thickening towards NW. Other major Miocene structures include NNE-striking wrench faults extending from the Mur-Mürz fault into the southern Vienna Basin. These faults include extensional sinistral strike slip duplexes and negative flower structures associated with Middle to Late Miocene growth strata (Hinsch et al., 2005a). Sinistral strike-slip faulting and pull-apart subsidence terminated during a major event of stress reorientation in the Upper Pannonian. Regional compressive stresses switched from N (NE)-S (SW) directed compression persisting through the Middle and Upper Miocene; Fodor, 1995; Häusler et al., 2002; Peresson & Decker, 1996) to E-W directed compression in the Pontian to Pliocene leading to an inversion of the basin and to NE-SW directed extension during Pliocene and Lower Quaternary (Fig. 3; Decker, 1996; Peresson & Decker, 1996; Decker et al., 2005).

Middle Pleistocene to recent fault kinematics resemble the kinematics during Miocene pull-apart formation as shown by geological, seismologic and geodetic data proving active sinistral slip along the fault with a velocity of about 1 – 2 mm/a (Decker & Peresson, 1998; Grenerzcy, 2002; Grenerzcy et al., 2000; Decker et al., 2005; Hinsch et al., 2005a). Appraisals of fault kinematics based on seismic data, tectonic geomorphology and Quaternary basin analyses show that the active fault system includes a major NE-striking sinistral displacement zone located at the SE border of the Vienna Basin, and several N- to NNE-striking normal faults branching off from the strike-slip system (Fig. 2). Quaternary activity of the latter is indicated by tilted and dissected Pleistocene terraces as well as by Quaternary basins, which formed in the hanging wall of several normal faults (Aderklaa, Obersiebenbrunn

basin, Fig. 4; Chwatal et al., 2005; Decker et al. 2005). All active faults are reactivated Miocene structures. Earthquake data show that historical and instrumental seismicity is restricted to the strike-slip system at the SE basin boundary.

In the southern Vienna Basin the strike-slip system is characterized by a negative flower structure underlying an up to 140 m deep Pleistocene Basin (Mitterndorf Basin, Fig. 4; Hinsch et al., 2005a; Salcher et al., submitted). Pleistocene basin subsidence is related to the reactivation of a Miocene extensional strike slip duplex at a releasing bend along the strike-slip fault in the southern part of the Vienna Basin (Mitterndorf-Schwadorf fault segment). Similar basins also occur along the NE continuation of the wrench fault referred to as the Lassee basin (Lassee segment, Fig. 4) and the Zohor, Pernek and Sološnica basin in the Slovak Republic (Fig. 15). The Lassee-Zohor basin with up to 100 m Pleistocene growth strata is situated some 20 km NE of the Mitterndorf basin. Both basins are separated by a fault segment, where strike-slip faulting is not combined with significant vertical movement (Arbesthal segment). Unlike the Mitterndorf-Schwadorf segment, the Arbesthal and Lassee fault segments show virtually no historical seismicity (Hinsch & Decker, 2003) although morphology strongly suggests Pleistocene faulting (Beidinger et al., submitted).

The current paper addresses a detailed analysis of fault geometries and kinematics of the Arbesthal and Lassee segment of the active Vienna Basin fault system using an ample 2D seismic grid provided by OMV Austria. This data is supplemented by 3D seismic covering part of the wrench fault. The results of seismic interpretation are compared to geomorphologic data highlighting the interaction between Pleistocene landscape evolution and tectonics.

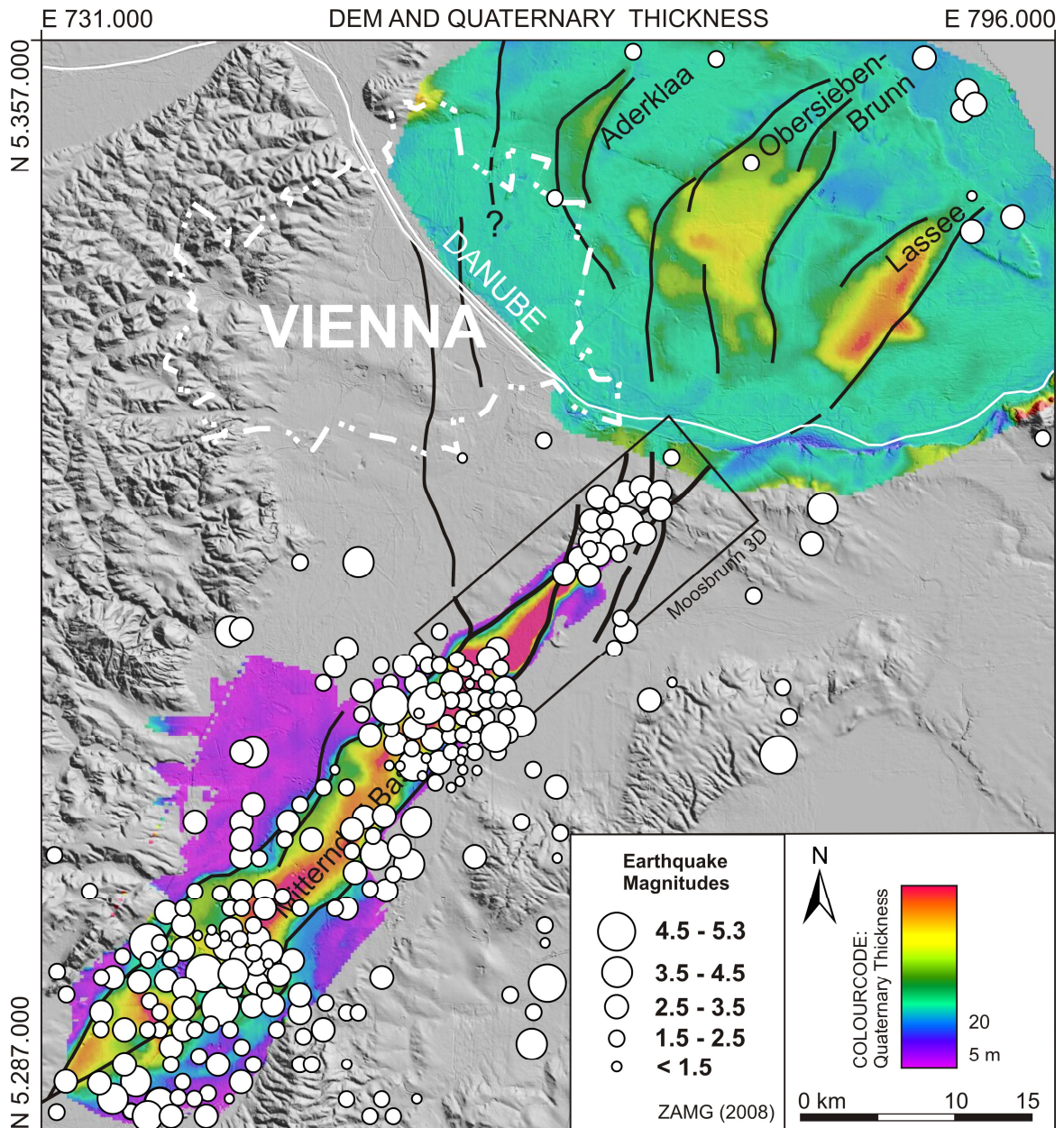


Fig.4. Quaternary faults, thickness of Quaternary deposits and earthquake epicenters (ZAMG, 2008) draped over a shaded digital elevation model of the southern and central Vienna Basin. Modified from Decker et. al., 2005 (see references therein for Quaternary database). Fault traces within 3D seismic "Moosbrunn" from Hinsch et al., 2005b.

3.2. Methodology

Seismic mapping of the Lassee Segment uses 2D industrial seismic data provided by OMV Austria covering the Lassee Basin and the adjacent Pleistocene terraces. The data consists of 3 inlines and 12 crosslines (Fig. 5).

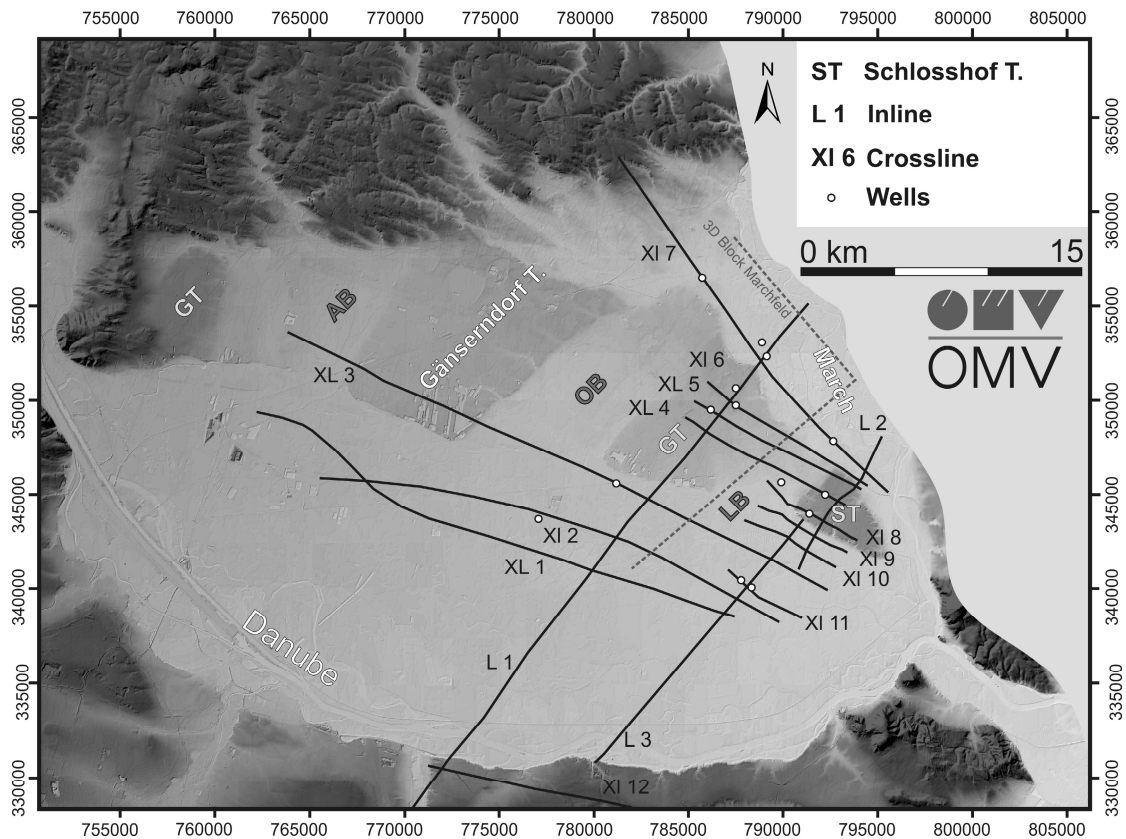


Fig.5. Seismic basemap on a shaded DEM of the central Vienna Basin north of the Danube. The Pleistocene terraces (GT, Gänserndorf terrace: Riss, c. 100 – 200 ky, Fink, 1973; Van Husen, 2000; ST, Schlosshof terrace) north of the Danube are cut by NE-trending fault scarps, which coincide with the boundaries of the Pleistocene Basins of Aderklaa (AB), Obersiebenbrunn (OB) and Lassee (LB; compare Fig. 4).

All sections are migrated time sections with a maximum recording time of 4 s TWT, which give high quality information down to about 3 s TWT. The 2D grid is supplemented by 3D seismic covering the northernmost part of the Lassee basin, which allowed for spatial fault mapping in a coherency cube. Data were integrated into a *Landmark Geografix* project. In this paper seismic sections are depicted to a maximum depth of 3.5 s TWT, which corresponds to about 6-7 km depth (Fig. 6 to 11). Seismic interpretation focused on Middle and Upper Miocene structures integrating borehole information and reflection

characteristics. Five stratigraphic horizons were mapped in all 2D seismic sections. The horizons are correlated to the general chronostratigraphic framework of the Vienna Basin (Central Paratethys Stages) using well data and sequence stratigraphic correlations (Fig. 3). The mapped horizons are characterized as follows:

Horizon in the Upper Pannonian (UP): The reflections of Upper Pannonian strata depict widely parallel and continuous reflectors with lower to medium amplitude. The mapped horizon exhibits a reflection with higher amplitude with respect to the others and has a thickness of about 20 - 30 ms. The horizon is not correlated to a particular chronostratigraphic level. It is easily mapped within the flower structure and in the fault block NW of it.

Top Lower Pannonian (TLP): The mapped horizon is correlated to the top of the Lower Pannonian stage by well control. The Lower Pannonian is generally depicted by a seismic facies with continuous reflectors of medium amplitude, which can be well correlated in the area NW of the SE boundary fault of the flower structure.

Top Lower Sarmatian (TLS): The Lower Sarmatian period is characterized by several regressions, which are probably reflected in the basinward shift of coarse sedimentation (Strauss et al., 2006; Harzhauser & Piller, 2004). The Top Lower Sarmatian is correlated to the youngest intense sea level drop (Strauss et al., 2006), which resulted in a chaotic reflection pattern of about 40 to 50 ms thickness with medium to high amplitudes. The horizon TLS is the youngest reflector, which can be traced all across the flower including the footwall block SE of the strike-slip fault. Stratigraphic correlations across the fault into the footwall block uses data of three wells (e.g., Fig. 7).

Top Aderklaa Conglomerate (TAC): The Aderklaa Conglomerate depicts a group of reflectors with a thickness of about 50 to 60 ms with very high amplitude. It corresponds to the lowstand system tract of the Early Badenian represented by fluvial facies with conglomerates (Kovac et al., 2004; Strauss et al., 2006). The TAC is overlain by a transgressive system tract with

reflectors onlapping the horizon. The top layer of the Aderklaa Conglomerate Mbr. is tied to several wells within the mapped seismic grid.

Top Pre-Neogene Basement (PNB): The pre-Miocene Basement in the investigation area consists of the allochthonous units of the Alpine-Carpathian thrust wedge. These include Mesozoic to Tertiary sediments of the Northern Calcareous Alps, Paleozoic units, and crystalline units with overlying Permo-Mesozoic cover (Kröll & Wessely, 1993). The PNB is characterized by reflections of medium to high amplitude and changing polarity generally showing a gentle relief. The depth of the PNB is constrained by several wells within the investigation area.

Time-depth conversions for estimating fault offsets and growth strata thickness use an empirically derived formula obtained from the comparison of borehole data and seismic sections in the Vienna Basin (OMV Austria):

$$Z = V_0(e^{kt} - 1) / k \quad (\text{Equation 1})$$

V_0 is the starting velocity [m/s], k is a constant tuning the increase of velocity with depth, and t is the OneWayTraveltime [s]. The parameters used for conversion in the Vienna Basin are: $V_0=1780$ m/s and $k = 0.7$ (Hinsch et al., 2005a).

Tectonic-geomorphologic analyses use the software ArcGis integrating data from seismic fault mapping, Pleistocene basin analyses and DEM data from the Central Vienna Basin.

3.3. Results and interpretation

3.3.1. Fault mapping

Regional fault mapping in the grid of fifteen 2D lines provided by OMV Austria focuses on Middle Miocene structures. All crosslines are widely consistent in showing about 3500 m thick Neogene sediments overlying pre-Neogene basement including 2000 to 3000 m thick Middle to Upper Miocene sediments and 500 to 1000 m of Lower Miocene successions below the Aderklaa Conglomerate Mbr. (horizon TAC).

The major structural element depicted in lines crossing the Lassee segment is an asymmetric negative flower structure, which includes Middle to Upper Miocene growth strata. The center of the flower coincides with the Quaternary depocenter of the Lassee basin (Fig. 6). Faults are shown as concave-up shapes in time sections whereas time-depth conversion results in mostly planar fault geometries. The asymmetry of the flower is indicated by horizons, which dip SE towards a major fault zone at the SE border of the structure. This fault zone accounts for a total vertical throw of the TAC and the Lower Miocene pre-growth strata of about 1300 m. It has a width of about 800 m including several splay faults spaced at distances of about 100 to 200 m (Fig. 9). These splays merge at the interface between pre-Neogene basement and the Neogene basement fill. The offset at the SE boundary of the flower structure is significantly higher than the cumulative vertical throw of about 400 – 800 m at its NW boundary. The general geometry of the flower structure is best depicted in section XL1 crossing the Quaternary Lassee basin in its central deepest part (Fig. 6).

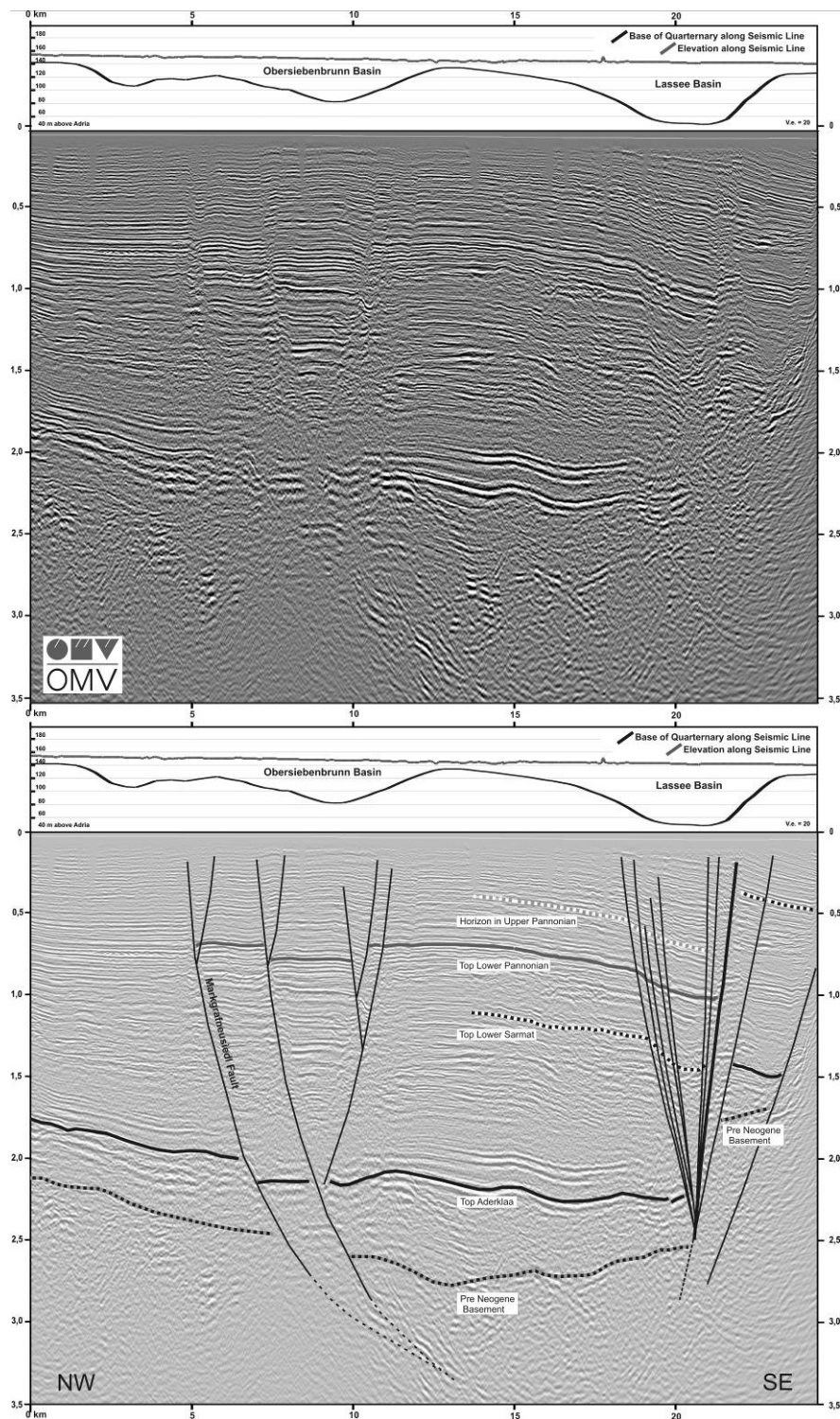


Fig. 6. Uninterpreted and interpreted seismic section XL1 across the Lassee flower structure (right; data by courtesy of OMV Austria). Note the general SE-directed dip of Middle to Upper Miocene strata towards the major fault zone delimiting the negative flower to the SE. Panels above show topography and Quaternary sediment thickness highlighting the Quaternary basins of Obersiebenbrunn (overlying the Markgrafenriedl normal fault) and Lassee above the flower structure. Quaternary growth strata of the Lassee Basin thicken. See Fig. 5 for location.

Although the general shape of the flower structure in the Lasse segment is consistent through all sections, comparison of the crosslines shows significant differences with respect to the number, arrangement and preferred dip directions of splay faults within the flower (Fig. 6 to 10). Observed differences also include the occurrence of minor splay faults dipping towards the fault, from which they branch off.

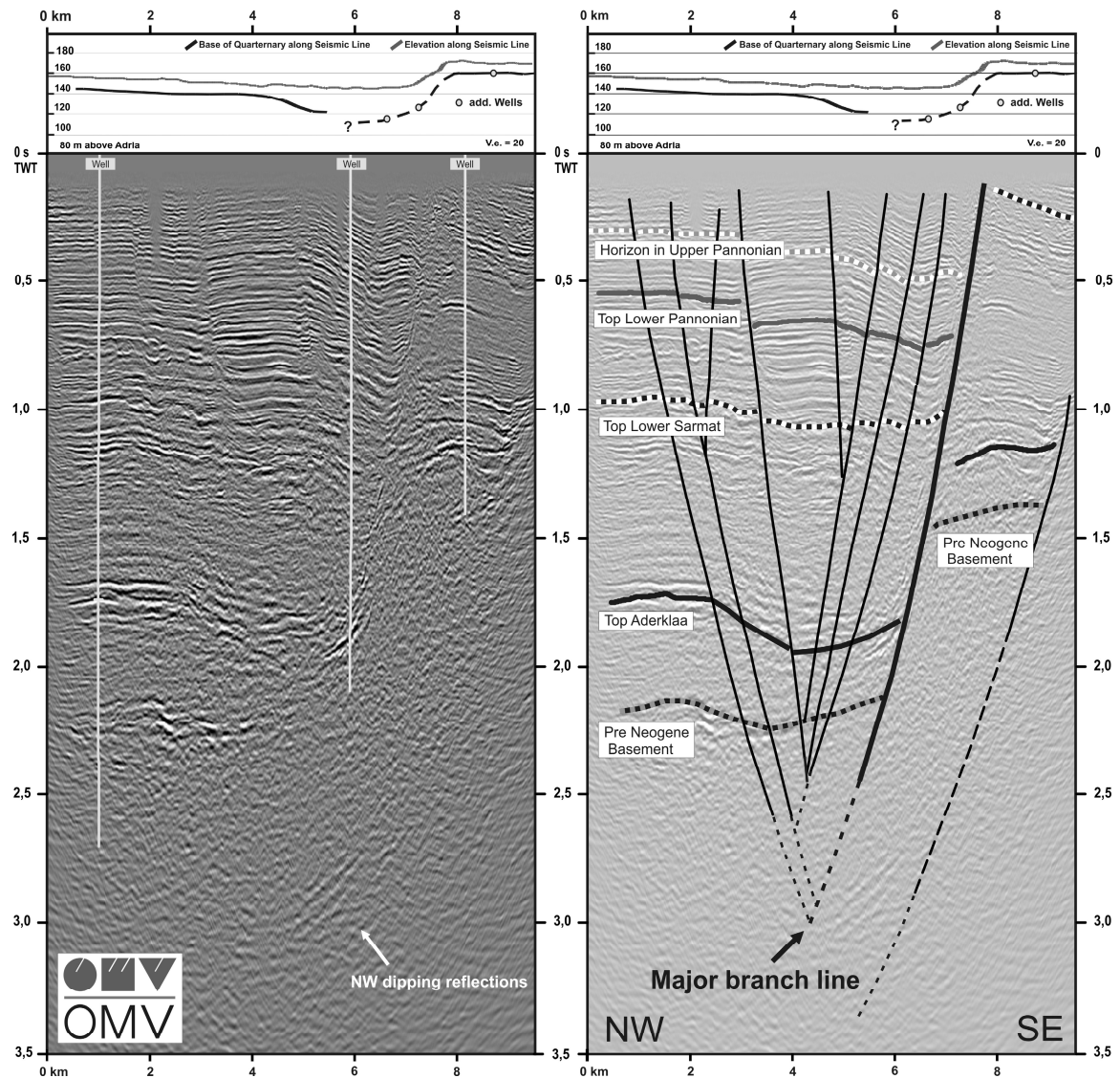


Fig. 7. The Lasse flower structure imaged in seismic section XL4. The SE-dipping topography of the gentle morphologic depression above the flower indicates tectonic control of surface topography. The SE margin of the Quaternary Lasse basin coincides with both, the up to 25 m high morphological scarp delimiting the Schlosshof Terrace and the major fault zone at the SE boundary of the flower. See Fig. 5 for location.

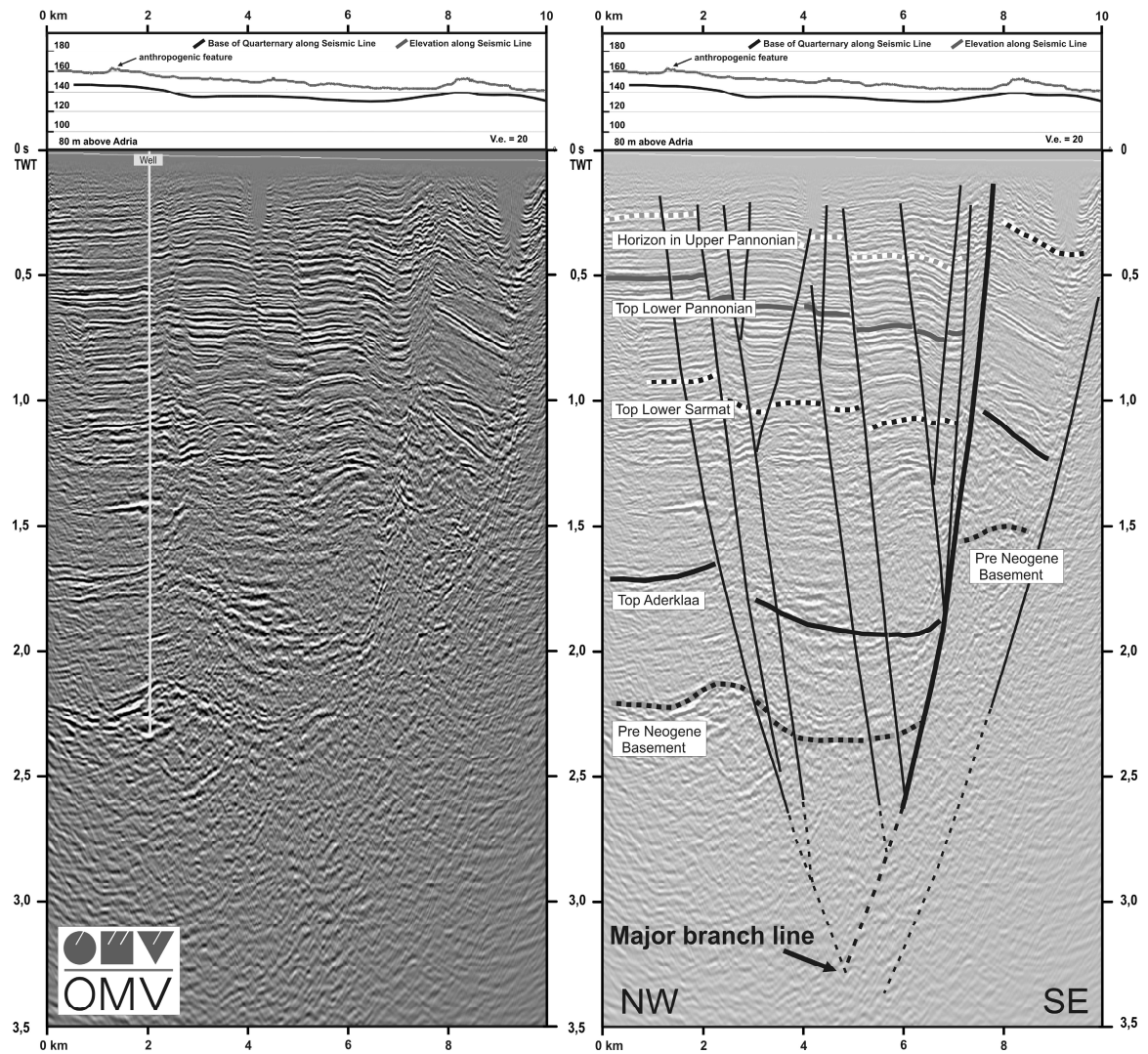


Fig. 8. Seismic section XL6 across the Lassee flower and the northern Lassee basin. Note surface topography dipping gently SE concordant with the tilt of Miocene strata in the flower structure and the position of the SE boundary fault of the flower below a morphological fault scarp. See Fig. 5 for location.

Detail Section XL 6

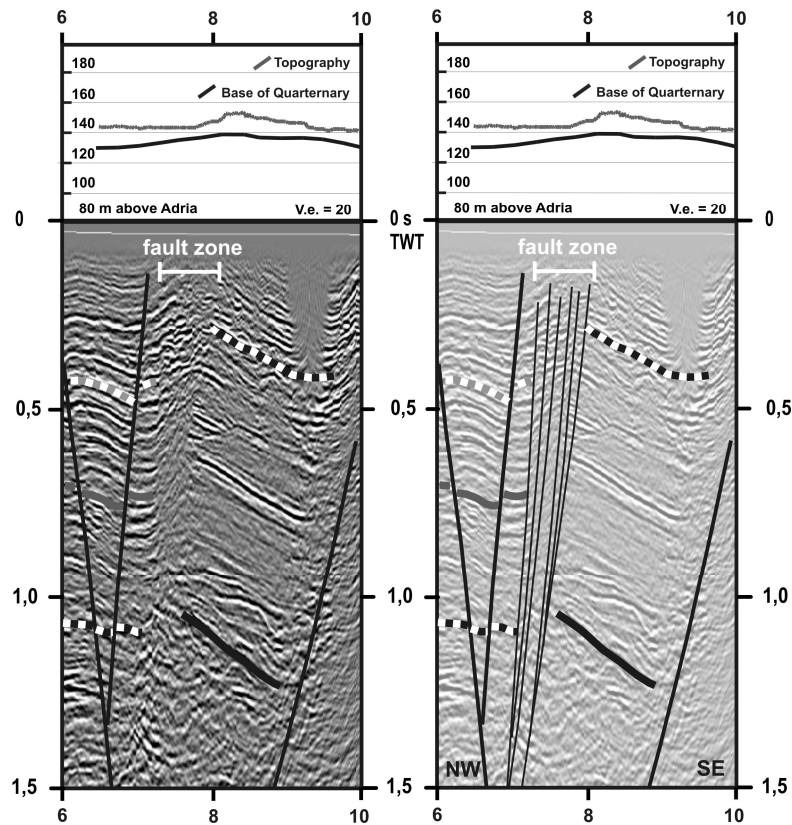


Fig. 9. Detail of seismic section XL 6 (Fig. 8) covering the fault zone at the SE boundary of the Lassee flower structure. The 800 m wide fault zone consists of numerous faults spaced at distances of 100 to 200 m well depicted in the uppermost 0.5 s TWT of the section. Short steeply NW dipping reflectors within the fault zone may indicate additional subseismic faults.

The flower structure consists of numerous splay faults, which converge to depth into a principle displacement zone (PDZ). We refer to the branch line, which approximately marks the top of the PDZ, as the major or first-order branch line (Figs. 6 to 10). It is mapped at the convergence of the outermost splay faults delimiting the flower structure both to the SE and NW. Mapping of this line through the 2D grid shows that it is located at a depth of about 3400 m below the center of the Lassee basin (XL1, Fig. 6). This depth roughly corresponds to the interface of the pre-Neogene basement with the Miocene strata. Crosslines north of XL1 show the first-order branch line at consistently increasing depth within the pre-Neogene basement. In these sections the down-dip continuation of faults below the horizon PNB is mapped from dip domains showing distinct SE-dipping and NW-dipping bundles of reflections, which terminate against the faults of the flower (Figs. 7, 10, 11). In the

northernmost section XL7 the major branch line is located at about 5500 m depth within the pre-Neogene basement (Fig. 10). These observations clearly indicate that the location of the first-order branch line is not controlled by the interface between pre-Neogene basement and Miocene basin fill (horizon PNB). Contrary to the first-order branch line, which dips towards NE, the horizon PNB is located at lower depth in the northern sections (2 s TWT, Fig. 10) than in the south (2.7 s TWT, Fig. 6). It is unclear whether the southeastern-most mapped fault, which is situated in the footwall block of the flower structure, is linked to the PDZ via a branch line at greater depth, or it is an independent normal fault not directly connected to strike-slip faulting. Terminating NW dipping reflections (Fig. 7, 10, 11) in the pre-Neogene basement indicate that the fault is not linked to the first-order branch line of the flower structure. The PDZ underlying the flower structure is not well imaged by seismic. Based on general tectonic models for the Vienna Basin it is thought to root in the basal detachment of the Alpine-Carpathian thrust sheets (Fig. 1b; Royden, 1985; Hinsch et al., 2005b).

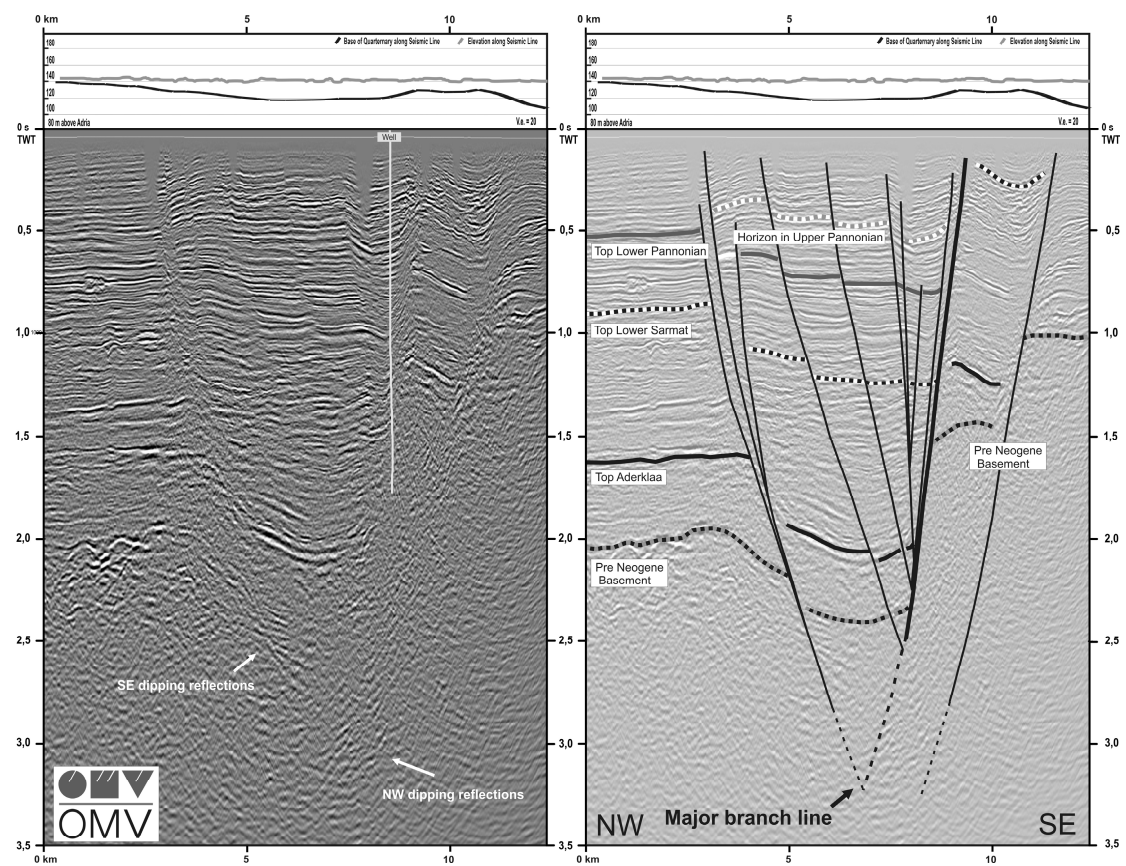


Fig. 10. Seismic section XL7 crossing the Lassee flower in the northernmost part of the Quaternary basin. Splay faults of the SE boundary fault mostly branch off at the interface between pre-Neogene basement and Miocene basin fill (horizon PNB). The first-order major branch line of the flower is located within the pre-Neogene basement. See Fig. 5 for location.

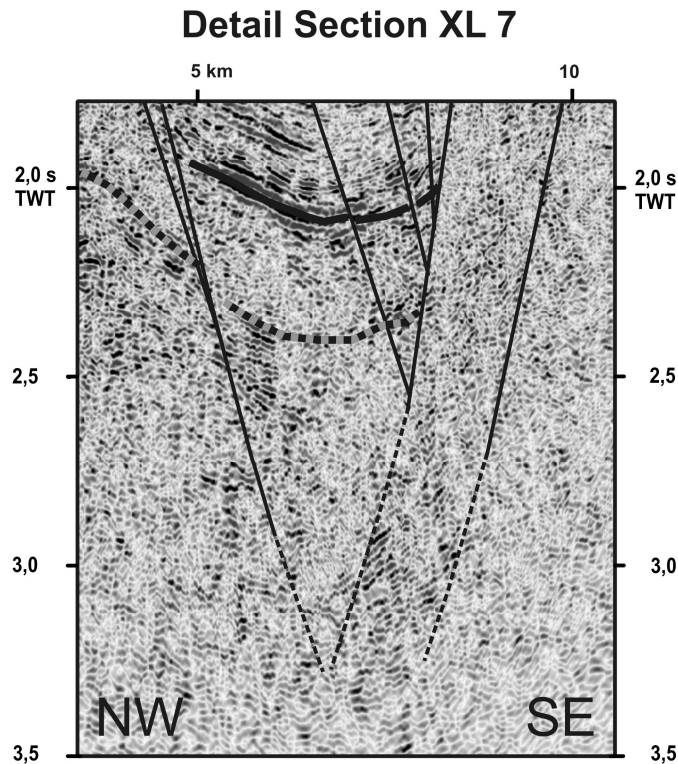


Fig. 11 Detail of section XL7 (Fig. 10) focusing on the first-order branch line of the flower structure above the principle displacement zone (PDZ). Sets of reflections dipping SE (at c. 2.5 s TWT) and NW (at 3 s TWT) allow tracing faults into the pre-Neogene basement and provide evidence for a deep-seated branch line at about 3.3 s TWT (~ 5500 m). NW-dipping reflections further indicate that the fault SE of the flower is not linked to this major branch line.

The branch lines of many splay faults are located at or close to the interface between the pre-Neogene basement (PNB) and the Miocene basin fill. This is observed for the first-order branch line in XL1 (Fig. 6) as well as for branch lines of lower order above the PDZ (Fig. 7, 10). The preferred occurrence of branch lines at the PNB presumably results from the significant change in rheology at this interface (Naylor et al., 1986; Richard et al., 1995). Additional branch lines occur in younger strata at the interface between Badenian and Lower Sarmatian strata (Fig. 7, 8, 10), which probably also forms a surface of significant rheological contrasts.

3.3.2. Growth Strata

The comparison of stratigraphic thicknesses of the Miocene sediments in the fault block NW of the flower structure, within the flower and in the block SE of it addresses an assessment of the timing of fault activity and the distribution of slip along the NW and SE boundary faults of the flower. The detailed analysis of growth strata for the time intervals Badenian-Lower Sarmatian and Upper Sarmatian-Pannonian further reveals significant differences in growth strata distribution related to changing fault slip rates.

Growth strata for the Badenian to Lower Sarmatian (i.e., between horizons TAC and TLS) could be determined separately for both sides of the flower in the sections XL4 to XL7 (Tab. 1). Subdivision of the flower into a NW and SE part uses the position of the first-order branch line. For the sections XL1 and XL2 Badenian to Lower Sarmatian growth strata thickness was only determined for the SE boundary fault with respect to the fault block NW of the flower. In these sections the first-order branch line is situated above the pre-Neogene basement and very close to the horizon TAC making it very difficult to map the horizon inside the flower structure.

Line	Total vertical displacement of horizon TAC (16.1 – 8 Ma)		Badenian - Lower Sarmatian vertical dis. (16.1 – 12.2 Ma)		U. Sarmatian – U. Pannonian vertical displ. (12.2 – 8 Ma)		
	Lassees flower vs. NW fault block [m]	Lassees flower vs. SE fault block [m]	Lassees flower vs. NW fault block [m]	Lassees flower vs. SE fault block [m]	Lassees flower vs. NW fault block [m]	Lassees flower vs. SE fault block [m]	
XL1	n.a.	1300	n.a.	350	n.a.	950	(1)
XL2	n.a.	1350	n.a.	200	n.a.	1150	(1)
XL3	n.a.	n.a.	n.a.	n.a.	n.a.	n.a.	(2)
XL4	250	1200	100	250	150	950	(3)
XL5	350	1250	200	350	150	900	(3)
XL6	350	1200	200	350	150	850	(3)
XL7	800	1400	500	300	300	1100	(3)

Table 1. Vertical throw at the NW and SE boundary faults of the Lassees flower structure estimated from growth strata and the total vertical throw of the horizon TAC (Top Aderklaa Conglomerate) forming the top of the pre-growth succession. Vertical displacements are measured for the two time intervals Badenian - Lower Sarmatian and Upper Sarmatian – Upper Pannonian.

(1) First-order branch line above PNB; throw at the SE fault determined from the depth of TAC in the NW and SE fault block. (2) TAC cannot be correlated into the flower structure. (3) First-order branch line below horizon PNB. n.a.: not analyzed due to uncertain or impossible stratigraphic correlation.

Results obtained for the SE boundary faults of the flower show growth strata of Badenian to Lower Sarmatian age with thicknesses ranging from about 200 m to 350 m for sections XL1 to XL7 (Table 1, Fig. 12). Post Lower Sarmatian growth strata for the SE boundary fault are not determined directly because Pannonian Stratigraphic horizons could not be correlated into the fault block SE of the flower structure. The amount of post-Lower Sarmatian vertical movement is therefore obtained from the difference between the total vertical throw of the fault measured for the horizon TAC (about 1200 to 1400 m; Table 1) and the Badenian to Lower Sarmatian displacement. Post-Lower Sarmatian vertical movements estimated from this approach are about 850 to 1150 m characterizing the displacement between the Upper Sarmatian and the late Upper Pannonian, which coincides with the onset of basin inversion (Fig. 3).

For the faults delimiting the flower to the NW Badenian to Lower Sarmatian (horizon TAC to TLS) growth strata indicate between 100 and 200 m vertical displacement with an increase of up to about 500 m in line XL7 (Table 1, Fig. 10). For the same reasons as described above, no data were obtained for the sections XL1 and XL2. Upper Sarmatian to Lower Pannonian growth strata for the NW boundary fault determined for the interval between the horizons TLS and TLP show about 50 m growth strata in the sections XL1 to XL6. Growth strata thickness increases to about 150 m in section XL7. Post-Lower Pannonian growth strata for sections XL4 to XL7 are again computed from the difference between total vertical throw and the thickness of older growth strata. Accordingly, about 100 m additional vertical movement occurred until late Upper Pannonian.

The growth strata estimates for both sides of the flower structure are summarized in Table 1 and Fig. 10. It is stressed that these data are related to uncertainties resulting from the decreasing resolution and seismic quality with depth, which makes it difficult to locate horizons exactly at greater depths. The used formula for time-depth conversion, which follows an exponential function (Equation 1), amplifies these picking errors with increasing depth. Furthermore the analysis of growth strata does not consider corrections for compaction as done by backstripping methods (Wagreich & Schmid, 2002; Hölzel et al., 2008). The determined offsets should therefore be considered as

approximations, which, however, are regarded sufficient for a general description of fault history.

The distribution of growth strata within the Lasseer flower structure accordingly shows that the fault accumulated only moderate displacement in the Middle Miocene (Badenian to Early Sarmatian) as indicated by total vertical movements of about 200 to 400 m during a time interval of about 4.1 Ma. Vertical displacements along the SE boundary faults of the flower are slightly higher than displacements on the NW fault, which shows an increase of vertical displacement along strike from S to N (Fig. 10). Fault slip rates between the Upper Sarmatian (12.2 Ma) and Upper Pannonian (basin inversion at 8 - 9 Ma), i.e., an interval of about 3.2 to 4.2 Ma, is significantly higher than in the Middle Miocene leading to vertical displacements of up to c. 1.150 m. The asymmetry of the flower shaped during that time by the concentration of displacement along the SE boundary fault. Vertical slip at this fault exceeds the displacement at the NW boundary by a factor of 10 (Fig. 12).

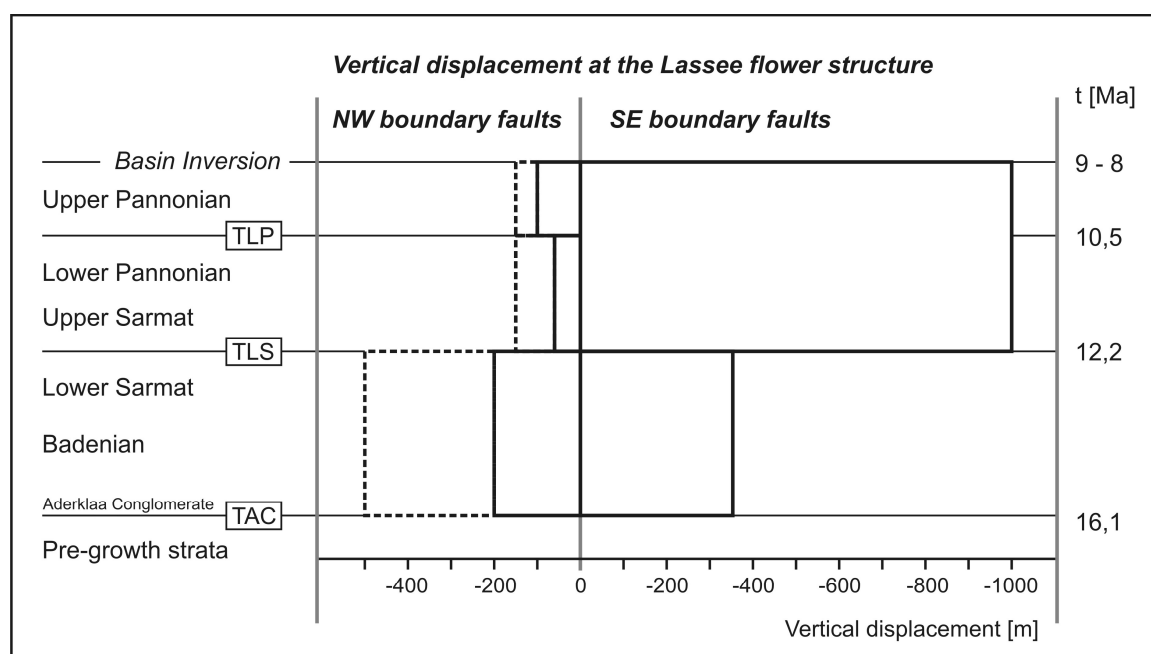


Fig. 12. Vertical displacements of the boundary faults NW and SE of the Lasseer flower structure with respect to the adjacent fault blocks outside the flower estimated from growth strata for the time intervals Badenian – Lower Sarmatian (TAC to TLS, c. 16.1 to 12.2 Ma) and Upper Sarmatian – Upper Pannonian (12.2 to 8-9 Ma). Indicated vertical displacements are mean values estimated from the seismic sections XL1 to XL6 (Tab. 1). Offsets at the NW boundary fault are shown separately for seismic section XL7 by the dashed rectangles.

3.3.3. *Geomorphology and Pleistocene basin evolution at the Lassesee fault segment*

The Lassesee basin with its up to 100 m Pleistocene growth strata overlies the central part of the Lassesee flower structure. The basin is located within the recent floodplain of the Danube river (Fig. 4). The shape of the basin mimics the asymmetry of the flower structure as shown by the base of Pleistocene gravels gently dipping towards the SE. Section XL1 across the center of the basin depicts an increase in Pleistocene sediment thickness towards the fault zone with maximum vertical offset at the SE boundary of the flower structure (Fig. 6). Such geometries are also evident from the sections XL5 and XL6 (Fig. 7, 8). Surface topography of those profiles, which are situated outside the floodplains of the rivers Danube and March (XL4 to XL6), shows that tilting towards the major fault zone also affects the recent surface reflecting the heterogeneous distribution of vertical offset in the flower in the Upper Pleistocene and Holocene (Fig. 7, 8).

The morphological boundaries of the northern part of the Lassesee basin are formed by the Gänserndorf terrace in the NW and Schlosshof terrace in the SE. These terraces are dated as pre-Würmian due to abundant cryoturbation and ice wedges as well as by Middle to Late Pleistocene mammal fossils found in the Gänserndorf terrace (Küpper, 1952; Thenius, 1956). Pre-Würmian age is also assigned to parts of the fluvial gravel within the Lassesee basin (Fuchs & Grill, 1984; Fink, 1973). No age data are available for the Schlosshof terrace, which is tentatively correlated to the Gänserndorf terrace by its similar facies of fluvial gravels and overlying palaeosol. Both Pleistocene terraces are delimited by marked morphological scarps facing towards the Lassesee basin. Scarps are arranged in right-stepping en-echelon patterns (Fig. 13a, b).

The northwestern, up to 25 m high, segmented morphological scarp of the Schlosshof terrace coincides with the fault zone with major vertical offset at the SE boundary of the flower structure (Fig. 7, 8). Borehole data indicate an increase in thickness of Pleistocene strata from about 8 m at the elevated part of the terrace to some 35 m below the scarp (section XL4, Fig. 5).

The segmented scarp of the Gänserndorf terrace NW of the flower differs from the Schlosshof scarp by its curvature. Steps in the topography and the base of Pleistocene sediments coincide with those faults at the NW side of the flower, which exhibit the maximum vertical offset of the horizon TLP (0.1 – 0.2 s TWT; Fig. 7, 8). In order to correlate these particular faults with morphology in 3 dimensions, the fault traces from seismic mapping were projected up to the surface. The piercing points of these faults plotted on the DEM are in line with the curved trace of the scarp of the Gänserndorf terrace (Fig. 13 a, b). Further information on fault geometries is obtained from a coherency timeslice of the 3D seismic Marchfeld at about 1.5 s TWT (c. 1800 m) depth. Data (Fig. 13 c, d) depict several curved fault traces. Two of these traces can be well correlated with the curved scarp segments at the surface.

The same procedure of projecting faults from 2D seismic was performed for the fault zone at the SE border of the flower structure. Piercing points follow the trace of the scarp of the Schlosshof terrace (Fig. 13 a, b). Segmentation of the scarp is related to the underlying fault zone, which includes numerous splay faults spaced at distances of 100 to 200 m (Fig. 9). Scarp segmentation results from the distribution of vertical offset to these splay faults, which apparently are linked by relay ramps. South of the Pleistocene terraces topography is controlled by the Holocene floodplain of the Danube river leaving no expressions of faults at the surface.

Both segmented scarps are interpreted to result from oblique sinistral shear within the underlying flower. The right stepping en-echelon faults were active during the Quaternary controlling the Pleistocene basin and landscape evolution. The faults are regarded as Riedel shears (Riedel, 1928) linked by relay ramps. A surface expression of such a relay ramp is found between the two scarp segments of the Gänserndorf terrace. Comparison of the topographic slopes of profiles along the relay ramp and across the fault-controlled scarp shows that the slope of the fault-controlled scarp is about 3.5 times higher than the average slope of the relay ramp (Fig. 13 e).

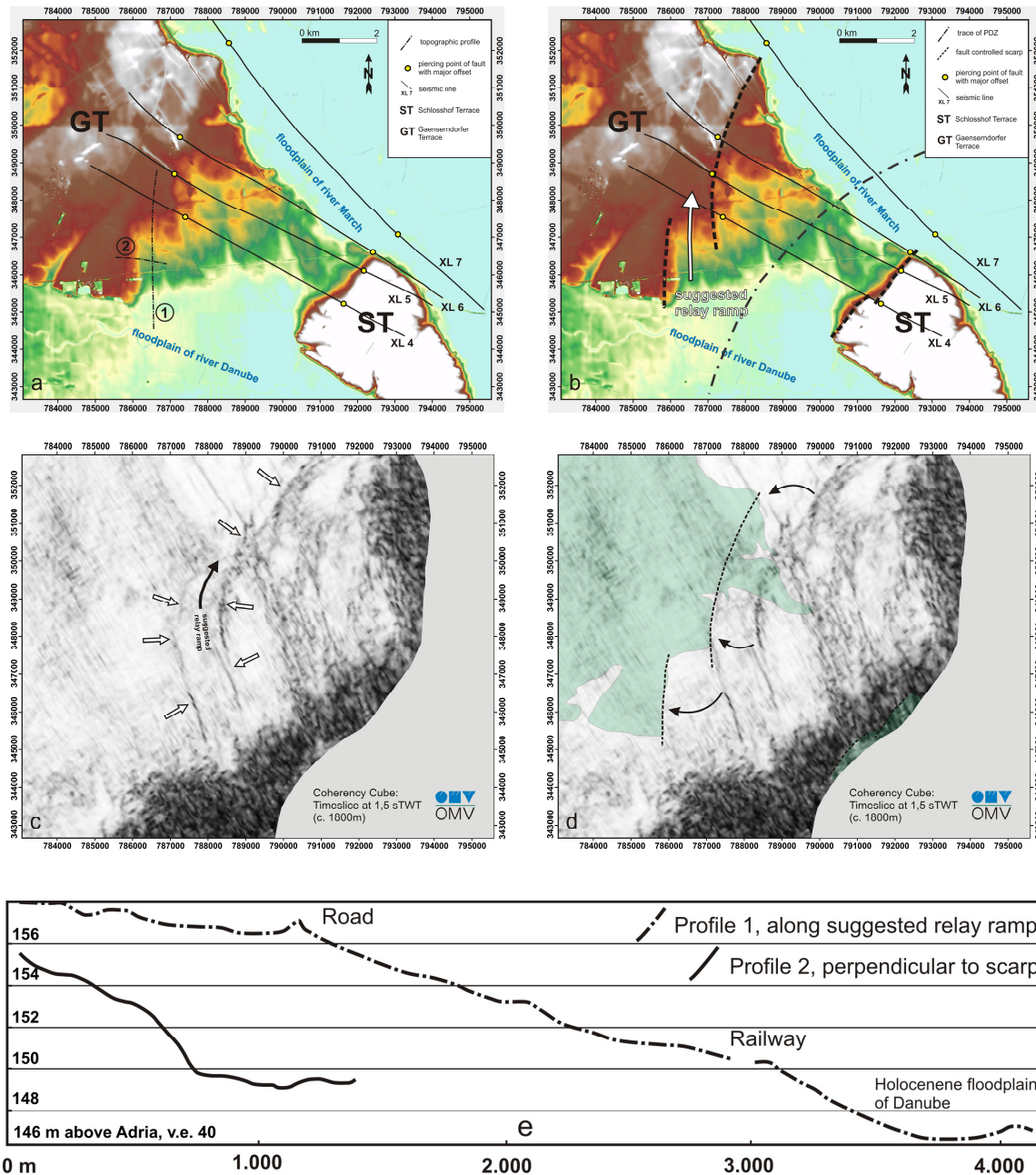


Fig. 13. (a, b) Digital elevation model of the Lassee basin and the adjacent Middle Pleistocene Gänserndorf (GT) and Schlosshof terrace (ST). Terrace boundaries facing towards the Lassee flower structure depict right stepping segmented fault scarps. Piercing points of fault traces mapped from 2D seismic (yellow dots) correlate with the morphological scarps.

(c) Coherency timeslice from the 3D seismic Marchfeld at 1.5 s TWT (about 1.8 km depth; by courtesy of OMV Austria) depicting the curved traces of two splay faults of the Lassee flower structure (white arrows). (d) Outline of the Gänserndorf terrace (green) combined with the coherency time slice. Projection of the curved faults to the surface (dotted curves) shows that both fault coincide with the topographic scarps E of the terrace. The faults are linked by a relay ramp.

(e) Profiles depicting topography of one of the fault-controlled scarps of the Gänserndorf terrace (2) and of the relay ramp (1) between the two faults at surface. The slope of fault scarp is about 3 times higher than the slope along the relay ramp. See (a) for location of the profiles,

Fig. 14 summarizes the geometry of mapped Riedel shears and the inferred PDZ in the northern part of the Lasse basin. Riedel shears with similar geometry are known from analog models where Naylor et al. (1986) revealed the formation of helicoidally shaped, en-echelon arranged Riedels in the overburden by moving a strike-slip basement fault underneath the undisturbed overburden. Riedel shear arrangement and helicoidal fault geometries are imaged as flower structures in cross-sections. Helicoidal faults are interpreted to result from the change of the spatial orientation of the main stress axes in the overburden. Stress directions change with distance to the basement master fault due to the shear stress induced at the interface between basement and overburden (Mandl, 1988, p. 142). For a sinistral basement fault with an extensional component, mechanical conditions lead to helicoidal Riedel shears with oblique-sinistral slip in the overburden. These Riedel shears are arranged in an en-echelon, right stepping pattern with intervening relay ramps (Schlische et al., 2002). The Lasse flower, however, appears more complex than the described experiments, as the interface between pre-Neogene basement and Miocene basin fill does not coincide with the depth of the first-order branch lines of the flower structure (Fig. 14 b).

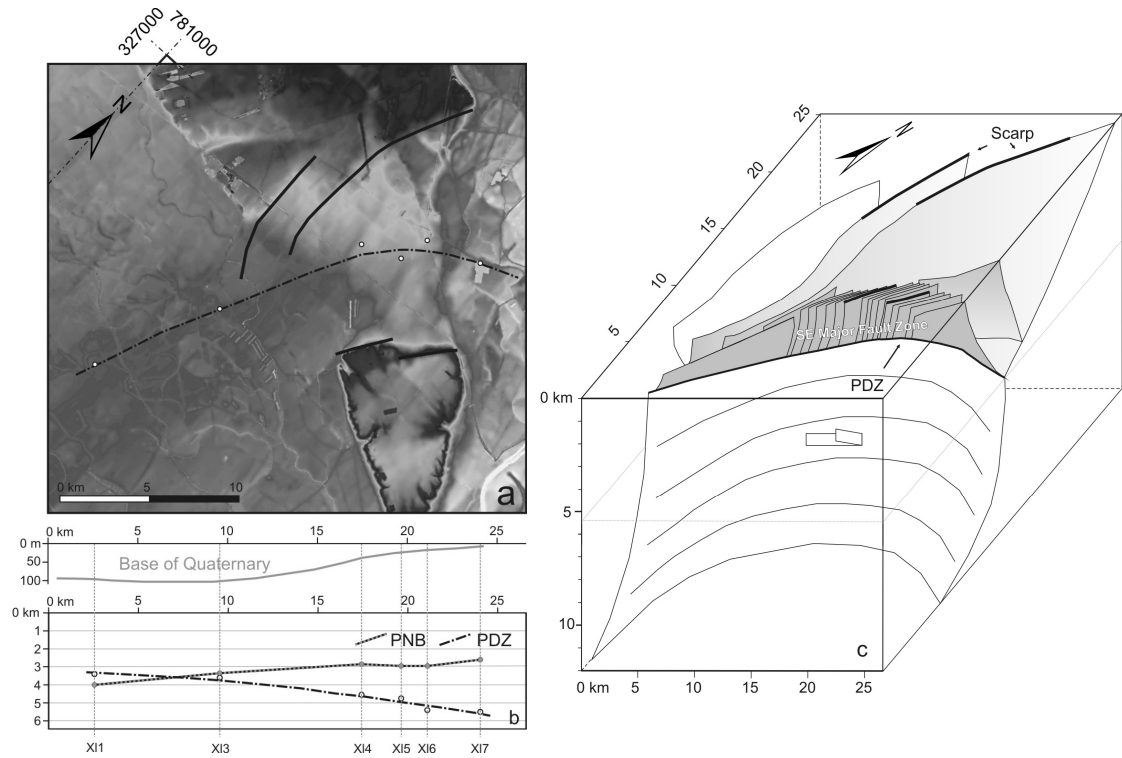


Fig. 14. (a) Surface-breaking faults of the Lassee flower structure and trace of the PDZ shown on a digital elevation model.

(b) Profile parallel to the strike of the PDZ of the Lassee segment. Base of Quaternary: thickness of Quaternary sediments in the Lassee basin above the PDZ; PNB: depth of the pre-Neogene basement; PDZ: top of the principle displacement zone derived from first-order branch lines of the overlying flower structure.

(c) Block diagram illustrating the geometry of the PDZ and the arrangement of en-echelon splay faults in the flower structure.

3.4. Discussion

3.4.1. *The Lassee Segment in a regional context*

The following paragraph addresses a discussion of the Quaternary and recent kinematics of the sinistral Vienna Basin fault starting from a reconstruction of the location and orientation of the PDZ of the fault, which is mapped using the first-order branch line of flower structures depicted in 2D seismic. Data from the Lassee segment are supplemented by sections covering the Mitterndorf Basin in the SE and the continuation of the Lassee segment to the NE. The resulting trace of the PDZ includes several fault bends delimiting seven segments, which differ in their strike directions. Segmentation defines releasing bends, which are associated with Peistocene basins (Fig. 15). From SW to NE, segments are characterized as follows.

The general strike of the Mur-Mürz segment SW of the Vienna Basin is ENE as deduced from geological data, morphology and the distribution of seismicity along the fault (Fodor, 1995; Gutdeutsch & Aric, 1988; ZAMG, 2008). The segment is not associated with extension and Miocene / Pleistocene basin formation indicating that its strike is parallel to the displacement vector. Within the Vienna Basin the fault zone includes the NE striking Mitterndorf-Schwadorf segment (1, Fig. 15) coinciding with the Pleistocene Mitterndorf basin and its underlying extensional duplex (Hinsch et al., 2005a; Salcher et al., submitted). The ENE-striking Arbesthal segment N of the Mitterndorf basin (2, Fig. 15) is not associated with Pleistocene basin formation. The Lassee segment (3, Fig. 15) again strikes NNE carrying the Lassee Pleistocene basin in the center of the flower structure overlying the PDZ. Towards the northern termination of the Lassee basin the trace of the PDZ bends from NNE to ENE in segment (4). Pleistocene sediment thickness decreases at this segment (compare Fig. 10).

The Zohor basin north of segment 4 includes up to 100 m thick Pleistocene sediments (Kullmann, 1966; Fendek & Fendekova, 2005) overlying a generally NNE- to NE-striking PDZ (segment 5, Fig. 15). This about 35 km long part of the PDZ (referred to as Zohor segment) includes 3 distinct

Pleistocene depocenters (Kullmann, 1966). These depocenters (Zohor-, Pernek- and Sološnica basin) may result from minor fault bends of the PDZ similar to the bend north of the Lasse basin forming releasing bends, which results in extensional strike-slip faulting.

Earthquake data indicate that the active Vienna Basin fault system continues into the Western Carpathians (Brezovské Karpaty Mts.; Fig. 2) northeast of the Zohor segment (segment 6; Fig. 14). Marko et al. (1991) describe the Brezová block, which is limited by two right-stepping sinistral faults, as a transpressive flower structure forming a push-up. We tentatively relate this positive flower structure to a restraining segment of the Vienna Basin fault system or to right stepover between the Zohor segment and the continuation of the fault into the Vah valley (Fig. 1).

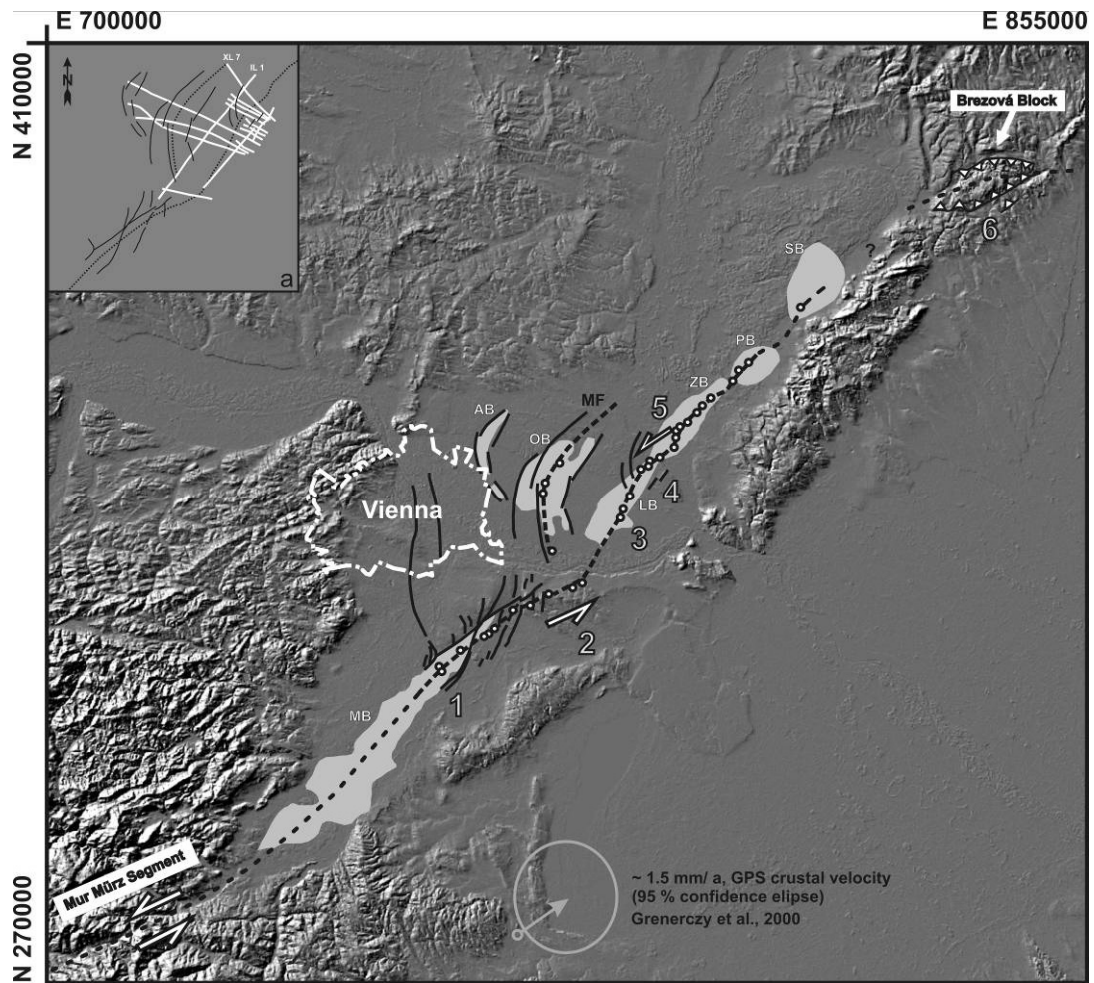


Fig. 15. Digital elevation model (SRTM data) of the Vienna Basin with outcrop traces of Quaternary faults. Pleistocene basins (light grey) are arranged along the Vienna Basin Transfer Fault at the southern boundary of the Vienna basin (MB: Mitterndorf Basin, LB: Lassee Basin: from Decker et al., 2005; ZB: Zohor Basin, PB: Pernek Basin, SB: Sološnica Basin, from Kullmann, 1966). Other basins overlie normal splay faults of the strike-slip system such as the Markgrafneusiedl fault (AB: Aderklaa Basin; OB: Obersiebenbrunn Basin). Outlines correspond to Quaternary sediment thicknesses of more than 40 m. White dots depict the position of the PDZ of the strike-slip system mapped from the first-order branch lines of the associated flower structures between 3 and 5.5 km depth, and the Markgrafneusiedl fault (MF) at the depth of the pre-Neogene basement. Dashed bold line: interpolated traces of the PDZ and the Markgrafneusiedl fault at the level PNB. Fault traces in the northern Mitterndorf basin from Hinsch et al., 2005b, fault traces along Obersiebenbrunn and Aderklaa basin modified from Decker et al., 2005. Insert: 2D seismic grid with fault traces.

3.4.2. The significance of normal branch faults (Markgrafneusiedl fault) for fault segmentation

Possible effects of splay faults on the segmentation of the Vienna Basin strike-slip system are discussed for the Arbesthal segment (segment 2, Fig. 15) between the Mitterndorf-Schwadorf and Lassesee releasing bends. This ENE-striking segment depicts kinematics, which differ from both adjacent segments. The estimated amounts of vertical offset shown in section XL12 (Fig. 16) are significantly less than those observed at the Lassesee and Mitterndorf-Schwadorf segment with about 600 m offset of the horizon Top Aderklaa Conglomerate (TOC). Growth strata show that most of the displacement occurred after the Lower Sarmatian (c. 100 m Badenian - Lower Sarmatian growth strata; about 500 m Upper Sarmatian – Upper Pannonian growth strata). The distribution of growth strata therefore is similar to that observed at the Lassesee segment (Tab. 1). Vertical offsets mainly occur at the NW fault strands.

The boundary between the releasing Mitterndorf-Schwadorf and the Arbesthal segment coincides with the branch line of the Markgrafneusiedl normal fault (Fig. 15). The fault is interpreted as an active fault as indicated by a Pleistocene basin overlying the fault and a marked fault scarp delimiting the Gänserndorf terrace (Fig. 4; Chwatal et al., 2005; Decker et al., 2005). Seismic section (XL1) crossing the Pleistocene Obersiebenbrunn basin shows that the basin is bounded by the Markgrafneusiedl fault and minor antithetic faults east of it (Fig. 6). Seismic mapping of the offset of fluvial channels serving as markers in Middle Miocene sediments in both the footwall and hangingwall of the fault prove normal fault slip (W. Hamilton, pers. comm.). The fault geometries in section XL1 (Fig. 16) resembling a negative flower structure are therefore not indicative for a strike-slip component. Seismic sections were used to map the trace of the normal fault at the top of the pre-Neogene basement (TNB). The branch point of this trace is located at segment (2) between the two releasing bends generating the Lassesee and Mitterndorf basin (Fig. 15). The fault is linked to the PDZ of the strike-slip system via a common detachment formed by the Alpine-Carpathian floor thrust (Hinsch et al., 2005b).

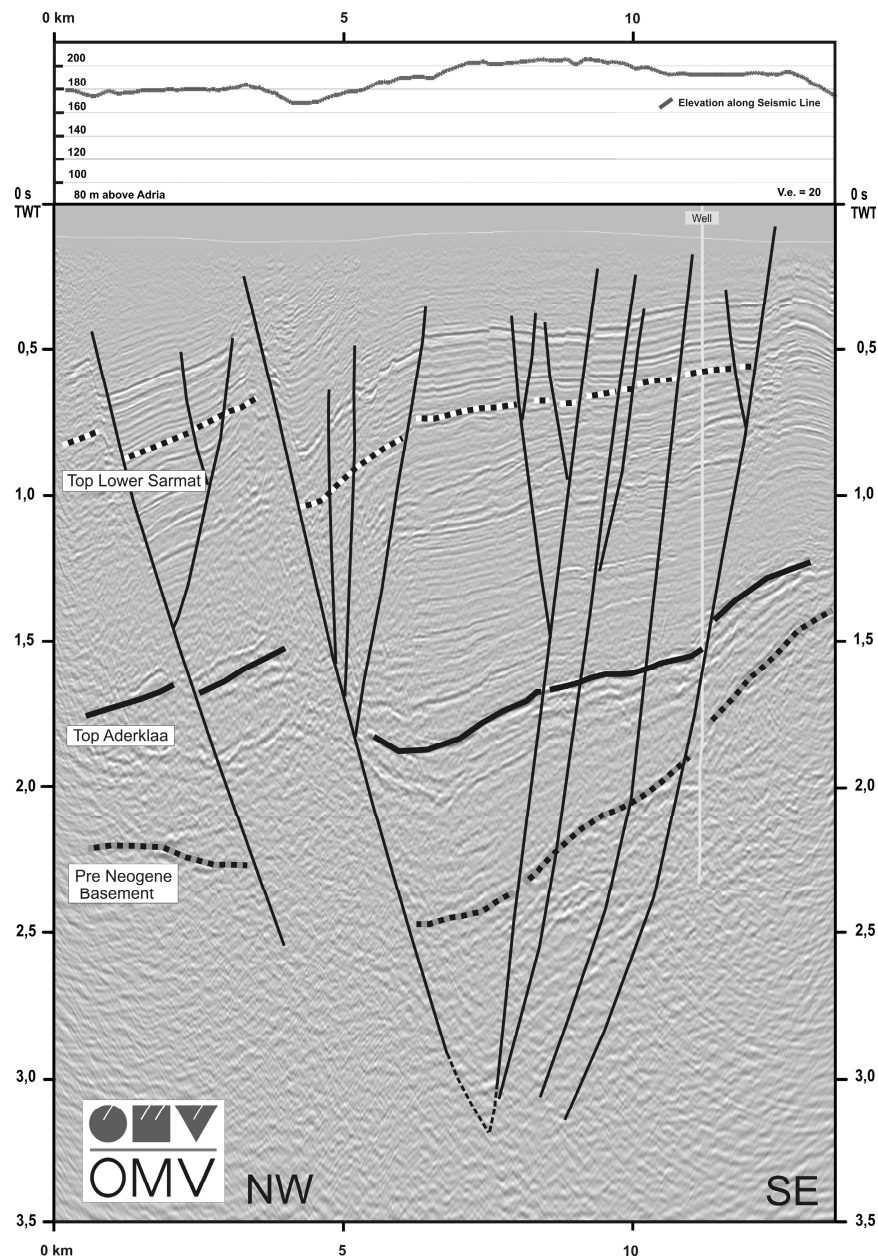


Fig. 16. Interpreted seismic section XL12 across the Arbesthal fault segment. The section crosses the strike-slip fault system between the Mitterndorf and Lassee Quaternary basin (see Fig. 3 for location). Asymmetry of the flower structure is distinct from the Lassee flower further north with growth strata thickening towards NW. Growth strata mostly occur in the uppermost 0.5 to 1 s TWT of the section above horizon TLS. The major vertical offset is significantly less than in the Lassee segment (600 m, horizon TAC) occurring at the NW boundary fault. Note the morphological scarp above the main fault at km 4 of the section.

A kinematic connection between the Markgrafneusiedl branch fault and the NNE-striking releasing bend along the Lassee Segment is indicated by the concurrent Quaternary activity of both faults. We suggest that part of the extension at the Lassee releasing bend, which includes an angle of about 35° with both the Arbesthal segment and the general slip vector of the Vienna

Basin fault system, is partitioned to the active normal faults. This assumption is corroborated by the observation that Quaternary normal faulting at the Markgrafneusiedl fault and its antithetic faults is restricted to those parts of the faults, which are located WNW of the Lassesee releasing segment as shown by the distribution of Quaternary sediments in the Lassesee basin (Fig. 15). Normal displacement at the Markgrafneusiedl fault and its antithetic faults diminishes both to the south and to the north of the Lassesee releasing bend (i.e., towards the non-releasing segments 2 and 4, Fig. 15).

3.5. Conclusions

Integration of 2D seismic data, Quaternary basin analyses and tectonic geomorphology studies identify the Lassesee segment as an active fault segment linked to a releasing bend of the Vienna Basin fault system. 2D seismic mapping of the Lassesee Segment depicts a negative flower structure with concave-up fault geometries in seismic time sections. These faults preferably merge in branch lines located at interfaces with significant rheologic contrasts. Such interfaces are located between the pre-Neogene basement and Miocene basin fill, and between Badenian and Lower Sarmatian strata. The first-order branch line, at which the NW and SE boundary faults of the flower structure merge into the underlying principle displacement zone, is situated at a depth of about 3.5 km in the southern part of the Lassesee segment. It dips towards NE to a depth of about 5.5 km within the pre-Neogene basement. This major branch line is regarded as the top of the PDZ. It is apparently not controlled by the rheologic contrast between the pre-Neogene basement and the Miocene basin fill.

Growth strata analyses indicate substantial fault movement during the Upper Miocene (Upper Sarmatian to Upper Pannonian) with up to 1150 m vertical offset along the fault zone at the SE boundary of the flower. These offset values differ significantly from offsets at its NW boundary, which do not exceed 250 m for the same time interval. The heterogeneous distribution of vertical offset within the flower structure results in an asymmetric shape with horizons dipping towards the SE boundary fault zone. This fault zone extends over a width of about 800 m and exhibits numerous splay faults spaced at intervals of 100 - 200 m.

Quaternary basin analyses and tectonic geomorphology depict continuous faulting during the Quaternary. The base of the Lassesee basin with up to 120 m thick Pleistocene sediments and the surface topography dip toward the SE border of the flower structure indicating that the general asymmetry of the flower controls both, Pleistocene basin geometry and recent surface topography. NE-trending morphological scarps delimit the Lassesee basin from

elevated Pleistocene terraces to the NW and SE. Both scarps are segmented depicting en-echelon, right-stepping geometries. All scarps coincide with faults, which exhibit significant vertical offsets within the underlying flower structure. The scarps are consequently interpreted as fault-controlled scarps resulting from underlying oblique-sinistral, en-echelon, right-stepping faults. The faults are interpreted as Riedel shears, which are linked by relay ramps and converge into common faults and the PDZ at greater depths.

Tracing the PDZ along the active fault zone at the SE boundary of the Vienna basin using the positions of the first-order branch lines mapped in seismic reveals several fault segments with different strike directions. NE- and NNE-striking segments act as releasing bends of the strike-slip fault system, which are associated with Quaternary basins. These segments differ from the ENE-striking ones striking parallel to the general displacement vector of the fault zone. The latter are not associated with Quaternary basins.

Among the releasing bends, the Lassee segment is apparently subject to higher extension values when compared to the NE-striking Mitterndorf-Schwadorf segment in the SW and the Zohor segment in the NE. The extension results from the higher angle between the Lassee segment and the general displacement vector of the strike-slip system. Excess extension seems to be accommodated by the Markgrafneusiedl fault and its antithetic normal faults located WNW of the Lassee basin. These faults also carry a Quaternary basin of significant thickness. The normal faults branch off from the strike slip fault at the fault bend of the PDZ between the Mitterndorf-Schwadorf and Arbesthal segment and merge with the Lassee segment at a common detachment.

4. The Lassee Segment of the Vienna Basin Fault System as a potential source of the earthquake of *Carnuntum* in the 4th century A.D.

4.1. Introduction

The Vienna Basin Fault System extends from the Eastern Alps through the Vienna Basin into the Outer Carpathians. It corresponds to a zone of moderate historical seismicity ($I_{\max} \leq 8.5$ corresponding to $M_{\max} \leq 5.7$; ACORN, 2004) with hypocenters mostly between 6 and 12 km depth (<12 km; ACORN, 2004; Lenhardt et al., 2007; ZAMG, 2008). The fault system consists of several sinistral strike slip segments with different kinematics and seismotectonic properties (Fig. 1; Fodor, 1995; Hinsch & Decker, 2003; Hinsch et al., 2005a; Hinsch et al., 2005b). Pleistocene basins, including the Lassee Basin and the Mitterndorf Basin at the Austrian part and the Zohor Basin at the Slovak part of the fault (Hinsch et al., 2005a; Salcher et al., submitted), are situated along the SE boundary fault of the Vienna Basin. These basins are interpreted to result from Pleistocene reactivation of Miocene faults in combination with local subsidence at releasing fault segments (Fig. 2; Decker et al., 2005). Seismic data provided by the OMV Austria depict negative flower structures underlying both the Mitterndorf and Lassee Basin (Decker & Peresson, 1998; Hinsch et al., 2005a; Beidinger et al., 2008).

Epicenter maps of the southern and central Vienna Basin show that seismicity is not homogenously distributed along the fault (Fig. 1). Moderate to relatively high seismicity at the Mitterndorf fault and in the Schwadorf region (including the earthquake of Schwadorf 1927, $I = 8$ / $M = 5.2$) and the Dobrá Voda segment (Dobrá Voda 1906, $I = 8.5$ / $M = 5.7$) differs significantly from the Lassee fault, which did not release significant earthquakes in the last centuries ($I < 6$ / $M \leq 3$) and appears as a locked or dormant segment (Fig. 1, 2; Hinsch & Decker, 2003). This is indicated by historical earthquake data, which are regarded complete for the last four centuries with regard to events with $I \geq 8$ (Grünthal et al., 1998; ZAMG, 2008). Comparison of seismic slip calculated from seismic moment summation therefore shows marked

differences between the individual segments of the Vienna Basin fault. Seismic slip of more than 0.7 mm/a at the seismically most active segments (Schwadorf and Dobrá Voda fault segment) strongly contrasts from slip rates close to zero at the Lassesee fault (Hinsch & Decker, 2003; 2008; Bus et al., in press). All segments, however, show marked slip deficits for the last century when comparing seismic slip rates with geodetic data and geologically derived slip rates of about 1 to 2 mm/a (Decker et al., 2005; Grenerczy, 2000, 2002).

In spite of the apparent extremely low seismicity in the last centuries the Lassesee fault is regarded as a possible source for the 4th century A.D. *Carnuntum* earthquake with an estimated intensity of $I_{loc} = 9 \pm 1$ (EMS-98). This earthquake was inferred from damaged Roman masonry recovered at the archeological site of *Carnuntum*, which is located about 10 km SE of the Lassesee fault (Kandler, 1989; Kandler et al., 2007; Humer & Maschek, 2007). Assessments of the seismotectonic scenario for this event point to a seismic source close to the damaged site as ground motion attenuation functions for the Vienna Basin fault system show a rapid decrease of local intensity with increasing distance from the epicenter (Decker et. al., 2006). For the *Carnuntum* earthquake remote seismic sources appear unlikely as a very high epicentral intensity ($I \geq 10$, corresponding to $M \geq 6$) would be required to explain the local damage at the archaeological site.

The current study therefore intends to provide data constraining the youngest fault history of the Lassesee fault. High-resolution geophysics (Ground penetrating radar), tectonic geomorphology techniques and geological investigations are used to trace suspected near-surface and surface breaking faults in order to prove or disprove Pleistocene and Holocene fault activity. The results of these combined studies lead to the discussion as to whether or not the Lassesee Segment is a possible source for the earthquake of *Carnuntum* 4th century, A.D.

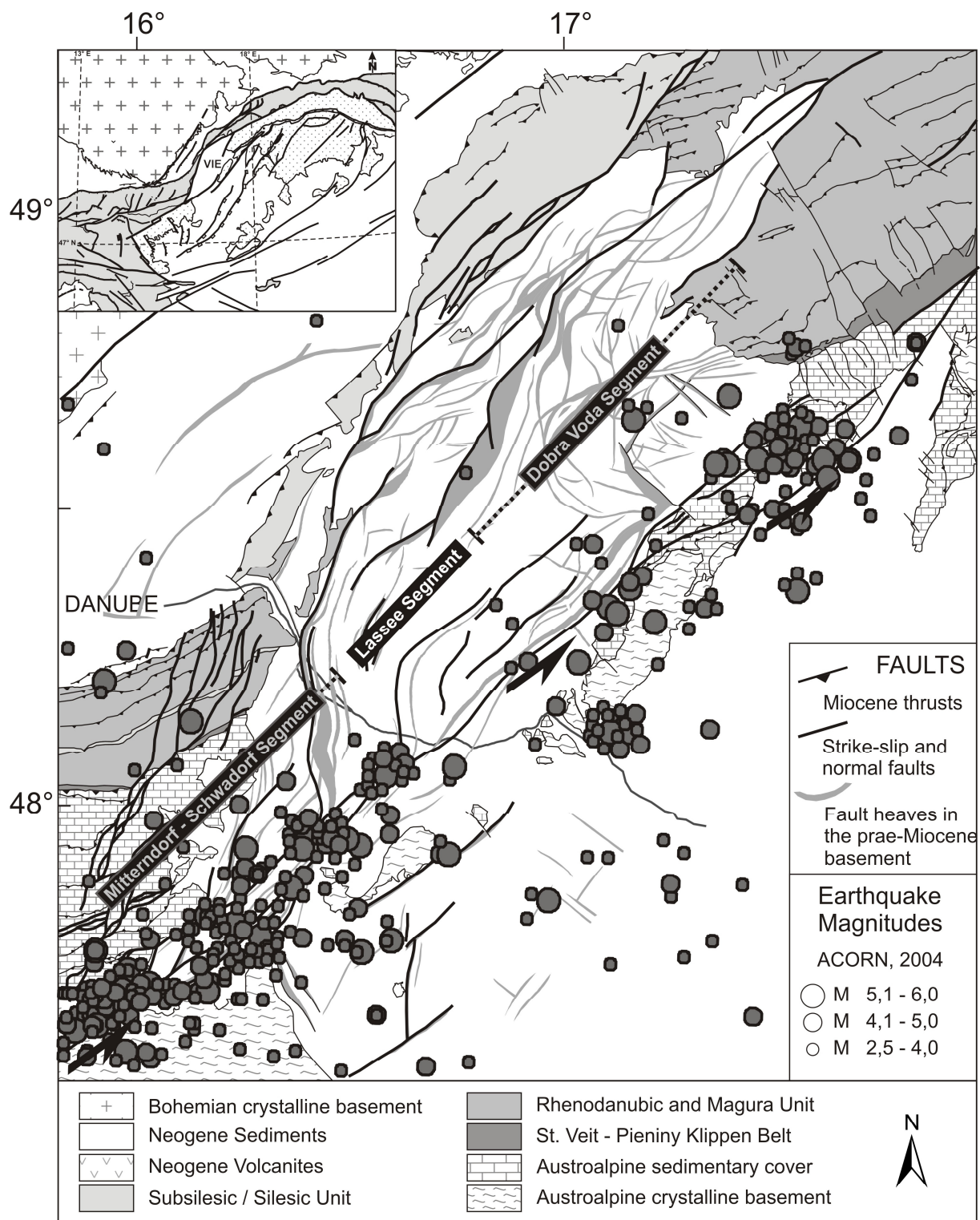


Fig.1. Tectonic map of the Vienna Basin highlighting Miocene faults of the pull-apart basin. Seismicity highlights the active sinistral fault at the SE basin margin. Insert map: Location of the Vienna Basin (VIE) in region between the Eastern Alps and West Carpathians. Fault heaves after Kröll & Wessely (1993).

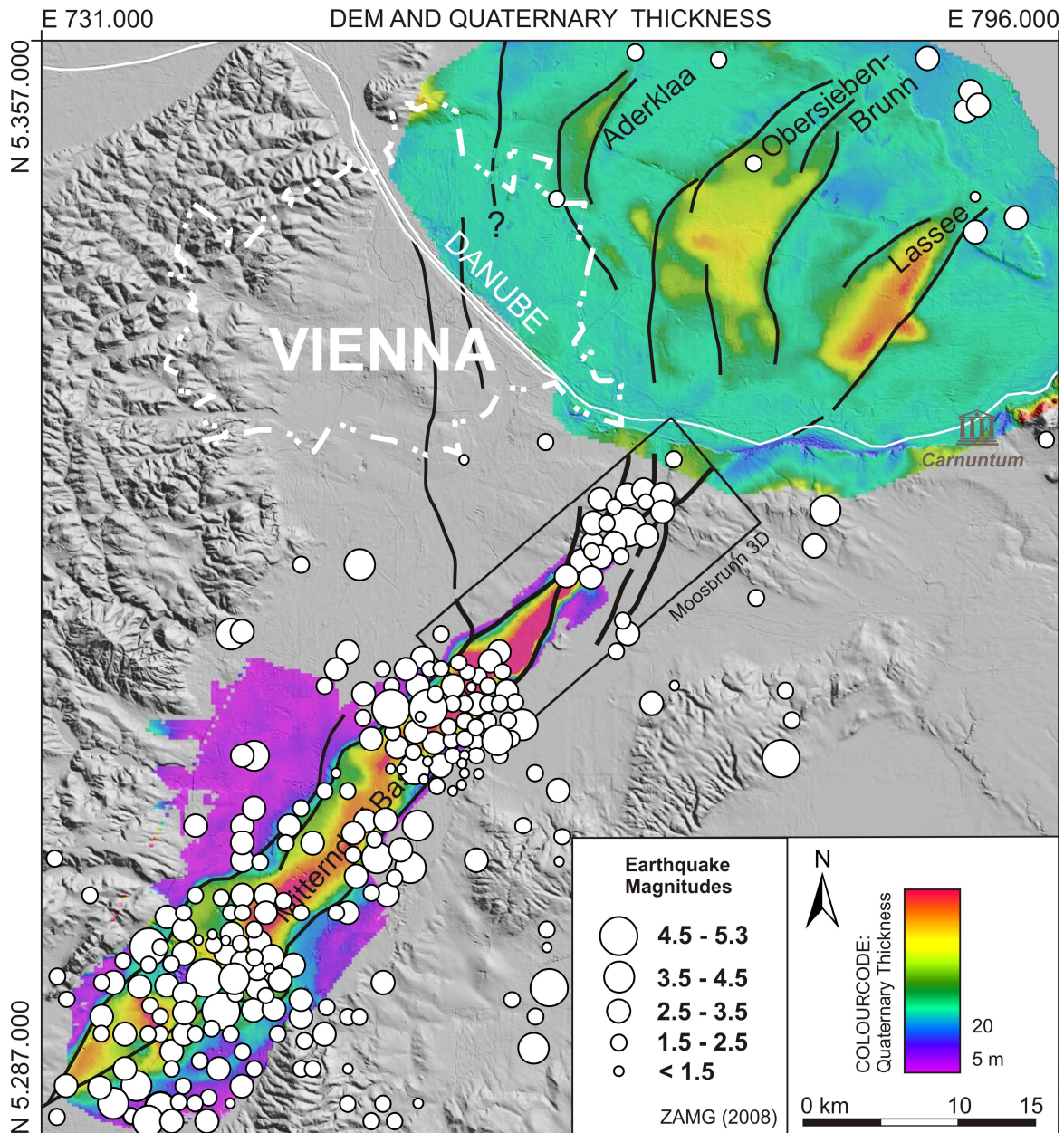


Fig. 2. Thickness of Quaternary sediments draped over a digital elevation model of the southern and central Vienna Basin (modified from Decker et al., 2005; Hinsch et al., 2005b). Quaternary Basins are delimited by active faults of the Vienna Basin Fault System. Note that seismicity is not homogeneously distributed along the fault system. The Lasseesee segment next to *Carnuntum* shows virtually no historical seismicity (earthquake data from ZAMG, 2008).

4.2. Geological background

Geomorphologic and geophysical investigations concentrate on scarps at the Lasse fault, which border the Pleistocene Schlosshof Terrace (Fig. 3). The terrace belongs to a group of fluvial terraces of the Danube river, which includes the Gänserndorf terrace further west. The terraces are transected by several NE-trending scarps, which are regarded as fault controlled features (Chwatal et al., 2005; Decker et. al., 2005; Fink, 1955).

Both terraces are composed of 10 to 20 m thick fluvial gravel with thin covers of red paleosoil and soil. Gravels are regarded as Upper Pleistocene (Riss, c. 120 - 200 ka;) dated by abundant cryoturbation and ice wedges confirming a prae-Würmian age, and Middle to Late Pleistocene mammal fossils found in the Gänserndorf Terrace indicative for Riss to Würm (Küpper, 1952; Thenius, 1956). No data are available for the Schlosshof Terrace, which was tentatively correlated to the Gänserndorf Terrace based on similar facies of both the fluvial gravels and the overlying paleosoils (Fink, 1955).

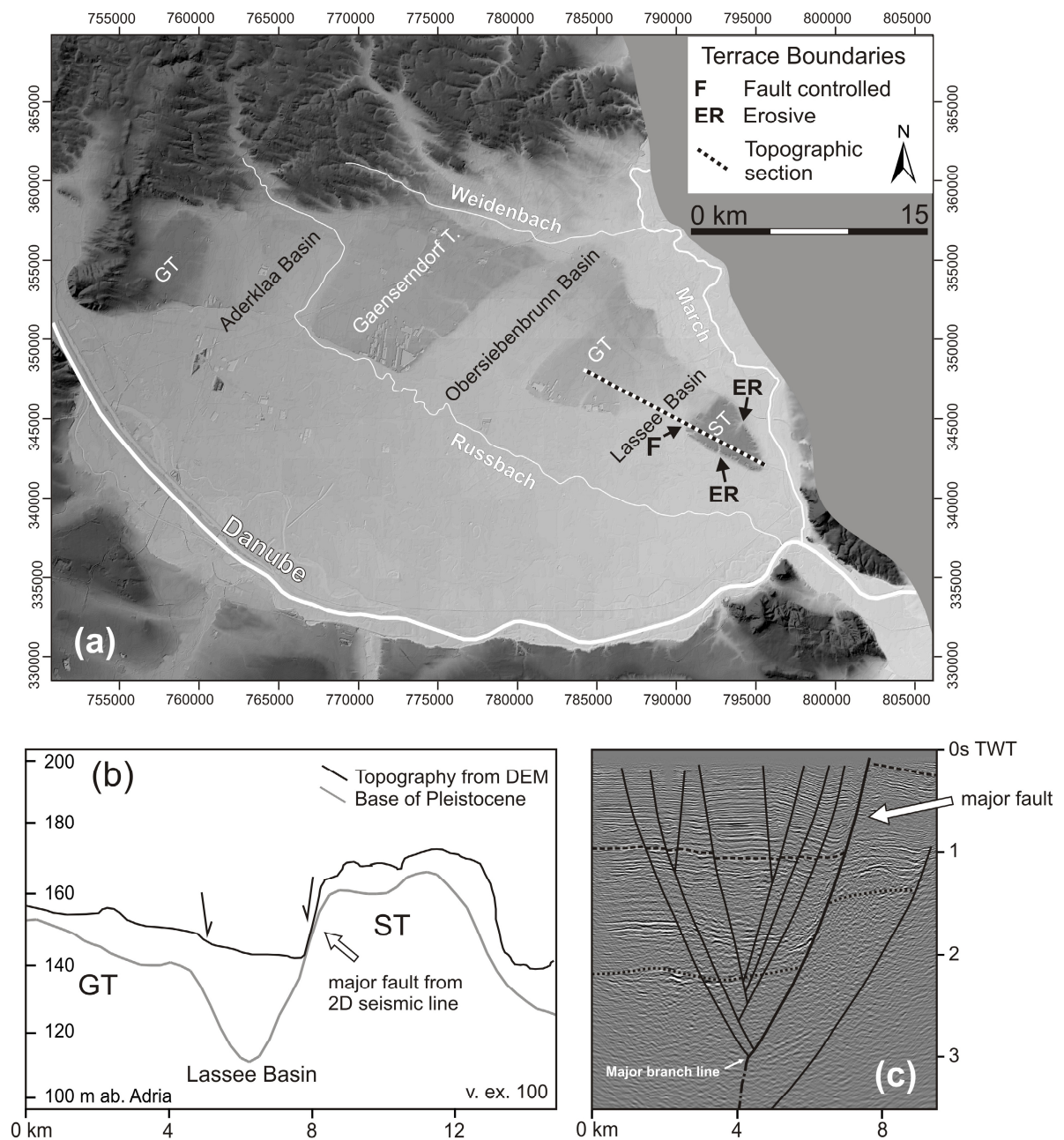


Fig. 3a. DEM of the Middle Pleistocene (Riss) Gänserndorf (GT) and Schlosshof Terrace (ST) of the rivers Danube and March. Erosive terraces boundaries (ER) delimit the plateaus from the Würm terrace and the Holocene floodplain of the rivers March and Danube. NE-SW striking scarps (F) are fault-controlled. Note that terrace boundaries coincide with the boundaries of Quaternary basins.

Fig. 3b. Topographic profile and Quaternary sediment thickness across the Lassee Basin.

Fig. 3c. Interpreted seismic section across the Lassee Basin depicting a negative flower structure underlying the Lassee Basin (dotted line: top of pre-Neogene Basement; dashed: Top of Lower Sarmatian strata; seismic by courtesy of OMV Austria).

Borehole data and a gravel pit indicate a Quaternary thickness of the elevated part of the Schlosshof Terrace from 7 to 10 meters (Fig. 4, 7). Outcrops in the gravel pit show a Pleistocene succession of braided river deposits mainly consisting of medium to coarse grained, partly imbricated gravel with sand and mica-rich matrix. Lenses of cross-stratified fine grained sand are intercalated with the gravels. Cryoturbation and ice-wedges occur in the upper two to three meters (Fig. 4). The Pleistocene sediments overlie fine-grained sand, silt and shale of Miocene age.

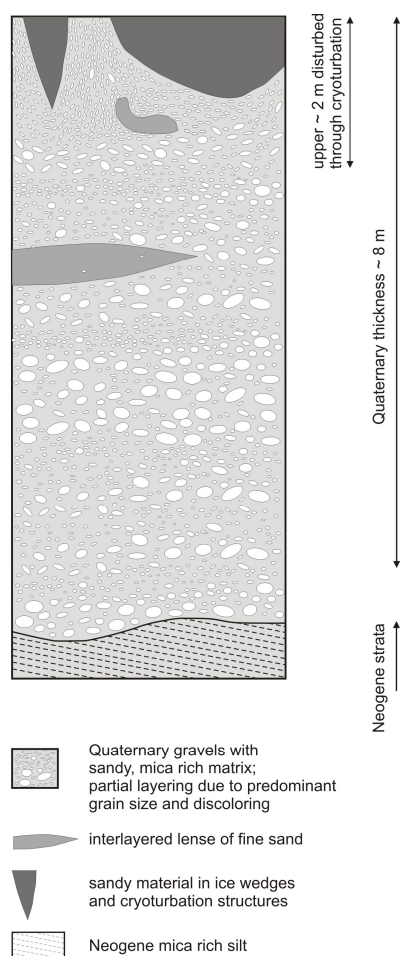


Fig. 4. Lithological profile of the Quaternary sediments of the Schlosshof terrace (see Fig. 7 for outcrop location). About 8 m thick fluvial gravel discordantly overlies fine-grained Miocene sediments. The upper 2 – 3 m include ice wedges and cryoturbation structures. Layering related to changes in grain size and sand content is depicted in 40 MHz GPR profiles. The top of Miocene aquiclude below the gravel corresponds to a strong GPR reflection.

NW of the morphological scarp, which delimits the terrace from the Lassee Basin, Pleistocene sediment thicknesses increase substantially as documented by well data (Fig. 7). Maximum Pleistocene sediment thickness in the center of the Lassee Basin reaches up to about 100 m (Fig. 2; Donaukraft Engineering, unpublished report).

4.3. Methodology

Ground penetrating radar was used to obtain high-resolution pseudo-images of sediment and deformation structures for the uppermost sediment layers from about 15 meters depth up to the surface. GPR depicts contrasts in electromagnetic properties (permittivity and electrical conductivity) of the investigated material. In the imaged sections such contrasts are produced by the partial layering and changes of the predominant grain sizes in Pleistocene gravels (Fig. 4), which are particularly well imaged by the 40 MHz surveys. The strong permittivity contrast between Pleistocene gravel and the underlying fine-grained Miocene sediments shows up as a strong reflection in these data.

To achieve both, a satisfactory exploration depth as well as an adequate resolution for uppermost sediment layers, two antennas with different center frequencies were used. The test assembly with a 40 MHz antenna combined with a 500 MHz antenna was previously applied by Chwatal et al. (2005) to trace the Markgrafneusiedl Fault in a similar geological environment. The period of investigation was during February and March 2007 in order to restrict side reflections, like from leafy trees, as part of the investigation area is situated in a forest. This appeared particularly important for recordings with the unshielded 40 MHz antenna (GSSI MLF Model 3200). Other possible sources of air reflections along the profiles such as power supply lines, fences, conifers, etc. were registered to avoid misinterpretations. The recording device was a GSSI SIR 3000 unit. The positions of all profiles were determined by using differential GPS, correction of topography was done by precession leveling as the elevations derived from differential GPS were not sufficiently accurate for processing the 500 MHz data records.

40 MHz measurements adduced a high exploration depth. The measurements were done in constant offset, in point mode with a point distance of 1 m. The main record data is: Time range=500ns, 1024 samples/scan, 16 bit/sample, static stack=32. All 40 MHz records were of good quality and therefore only moderate processing like the application of 1D and 2D filters and topographic

correction was necessary. Time values are converted to depth using an average velocity of 0.1 m/ns.

To get resolution in a range of tens of centimeters and information up to the uppermost decimeters, all of the 40 MHz sections first were covered by measurements with a 500 MHz antenna in zero offset and in continuous mode (main record data: 16 scans/s, time range=100ns, 1024 samples/scan, 16 bit/sample, marker interspace = 5m). Additionally to this, continuous mode survey measurements with the 500 MHz antenna were done in a point mode with a point distance of 0.1m. In comparison with the continuously measured sections the point wise measured ones, show much better record quality. The most probable reason for that is the very rough, bumpy terrain and therefore the difficulty of steering the antenna smoothly with a certain velocity. As for the 40 MHz data only minor processing like using 1D and 2D filters was necessary. After migration we found that migration in our case does not add information but reduces preferable resolution. Therefore the sections finally are presented without migration.

The interpretations of GPR data include independent geological subcrop data from the well database HADES (by courtesy of the Government of Lower Austria) providing lithologic and stratigraphic information from several hundred boreholes in the study area. Three groundwater tubes were used to determine the depth of the groundwater table at the time of GPR data acquisition. These wells also provided detailed data on the Pleistocene aquifer as well as on aquifers within the underlying Miocene sediments.

GPR fault mapping is supplemented by tectonic geomorphology studies using a DEM with 10 m horizontal resolution, morphological field mapping, and a 3D precise leveling survey covering a hanging valley, which cuts the fault scarp at the NW border of the Schlosshof Terrace.

All data were processed and integrated into an ArcGis project.

4.4. Results and interpretation

4.4.1. *Tectonic geomorphology*

Geomorphologic analyses use the Middle Pleistocene terraces of the rivers Danube and March as topographic markers, which are referred to as the Gänserndorf and Schlosshof Terrace (Fig. 3a; Fink, 1955). Both terraces are well depicted as shallow and extremely flat plateaus in the DEM. Approximately WNW-trending terrace risers delimit these morphological plateaus from the Würm terrace and the Holocene floodplains of the Danube and its tributary creek Russbach in the south as well as from the floodplain of the river March and its tributary Weidenbach in the north (Fig. 3a).

DEM data further show that the terraces are strongly dissected by marked NE-trending morphological scarps, which all but one are not related to surface runoff channels. These scarps coincide with the boundaries of Quaternary basins with up to 100 m thick Pleistocene to Holocene sediments and therefore have been interpreted as fault-controlled features (Fig. 3b; Fink, 1955; Chwatal et al., 2005; Decker et al., 2005).

Geomorphologic analysis focused on the triangular Schlosshof Terrace between the conjunction of the Holocene floodplains of the rivers March and Danube (Fig. 3a). The terrace has a widely planar surface forming an elevated plateau some 25 to 30 m above the surrounding areas, which gently dips against the slope of the Danube (Fig. 3b). Its overall triangular shape results from the erosive terrace risers to the NE and S, and from the fault-controlled scarp adjacent to the Lassee Quaternary Basin NW of the plateau (Fig. 3b, c). The latter is composed of two sub-parallel NE-trending partly overlapping morphological scarps, which are arranged in an en-echelon like right-stepping pattern (Fig. 5, 7).

Terrace risers and the fault-controlled scarps NW of the Schlosshof plateau differ by the morphology of shallow dry valleys dissecting the escarpments (Fig. 5). Profiles along the thalweg of dry valleys crossing the fault-controlled scarps depict hanging valleys with marked knickpoints in the valley floors

resulting from tectonic subsidence outweighing erosion by ephemeric floods (HV1 to HV4, Fig. 6). Such knickpoints occur in all valleys crossing the fault-controlled scarp. The dry valleys crossing the terrace risers are characterized by straight gently sloping valley floors devoid of significant knickpoints. Exceptions (valleys RD 3, RD 5 and MB, Fig. 6) are related to the backward erosion of perianual or ephemeric springs at the interface between Quaternary gravels and the underlying Tertiary aquiclude.

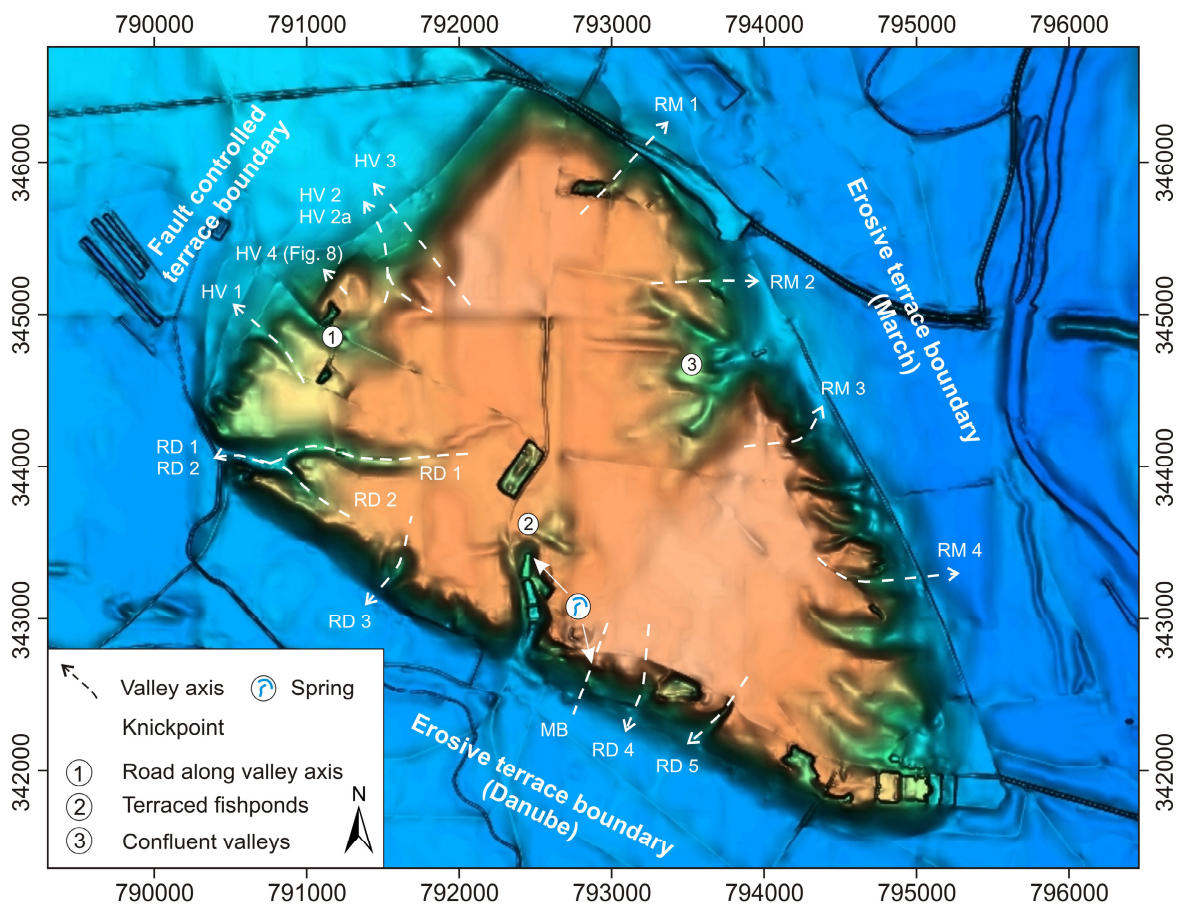


Fig. 5. Colored DEM of the Schlosshofer terrace with the location of topographic profiles along valley axes cutting the terrace boundaries. Topographic profiles are shown in Fig. 6.

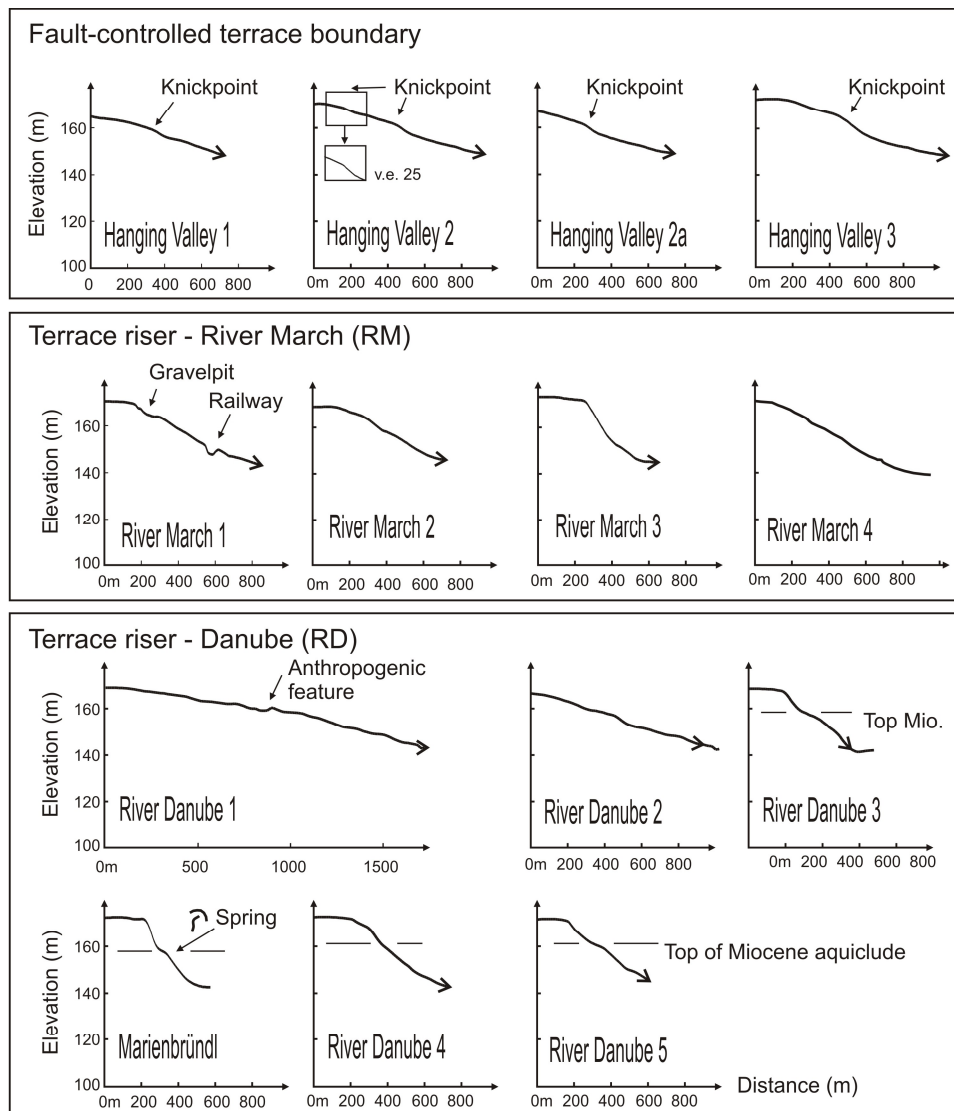


Fig. 6. Topographic sections along the axes of valleys crossing the boundaries of the Schlosshof Terrace (see Fig. 5 for locations). Valleys crossing the fault-controlled scarp show knickpoints characteristic for hanging valleys. Note that similar steps do not occur in valley floors facing the river March. The hanging valleys also differ from stepped valleys facing the Danube, which result from backward erosion of springs emerging at the top of the Miocene aquiclude.

Hanging valley topography is analyzed in detail for the valley HV 4 (Fig. 8 to 10) crossing the NW terrace boundary. Analyses use a high-resolution DEM derived from precise leveling with data covering an area of about 20.000 m² with 9 profiles parallel and another 9 profiles perpendicular to the scarp (Fig. 9). The profiles are spaced at distances of 10 to 20 m with leveling points at 0.25 to 0.5 m distance depending on the actual relief. The DEM shown in Fig. 8 results from natural neighbors interpolation gridding. High-resolution topography shows that both flanks of the valley and the valley floor are

crosscut by a marked NE-trending linear scarp of about 50 cm height paralleling the general trend of the terrace boundary.

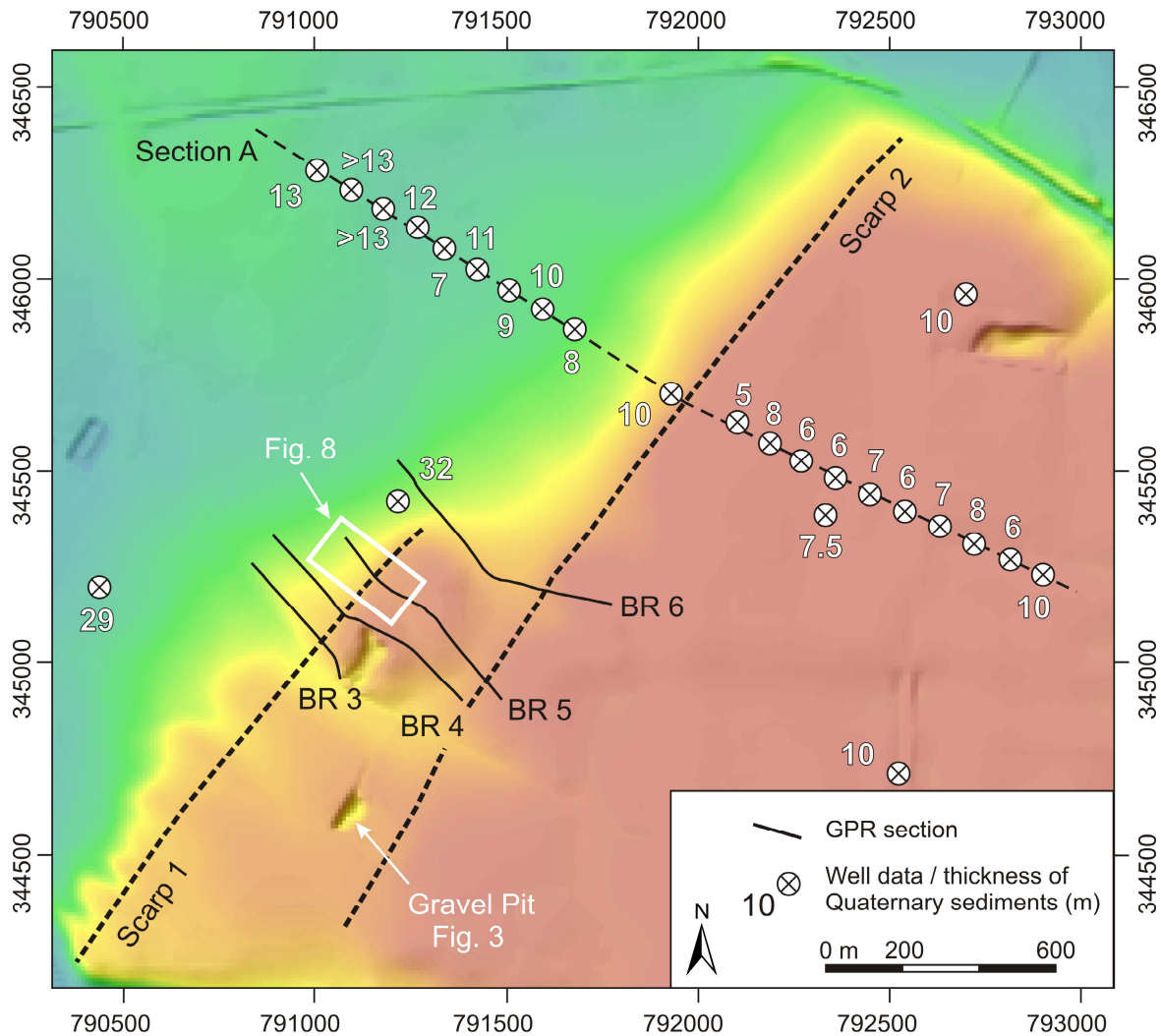


Fig. 7. Colored DEM of the NW part of the Schlosshof Terrace depicting two subparallel morphological scarps (black dashed lines) arranged in an en-echelon like pattern. The scarps overlap at the locations of GPR sections BR5 and BR6. Note the increase of Quaternary gravel thickness below the scarp indicated by borehole data.

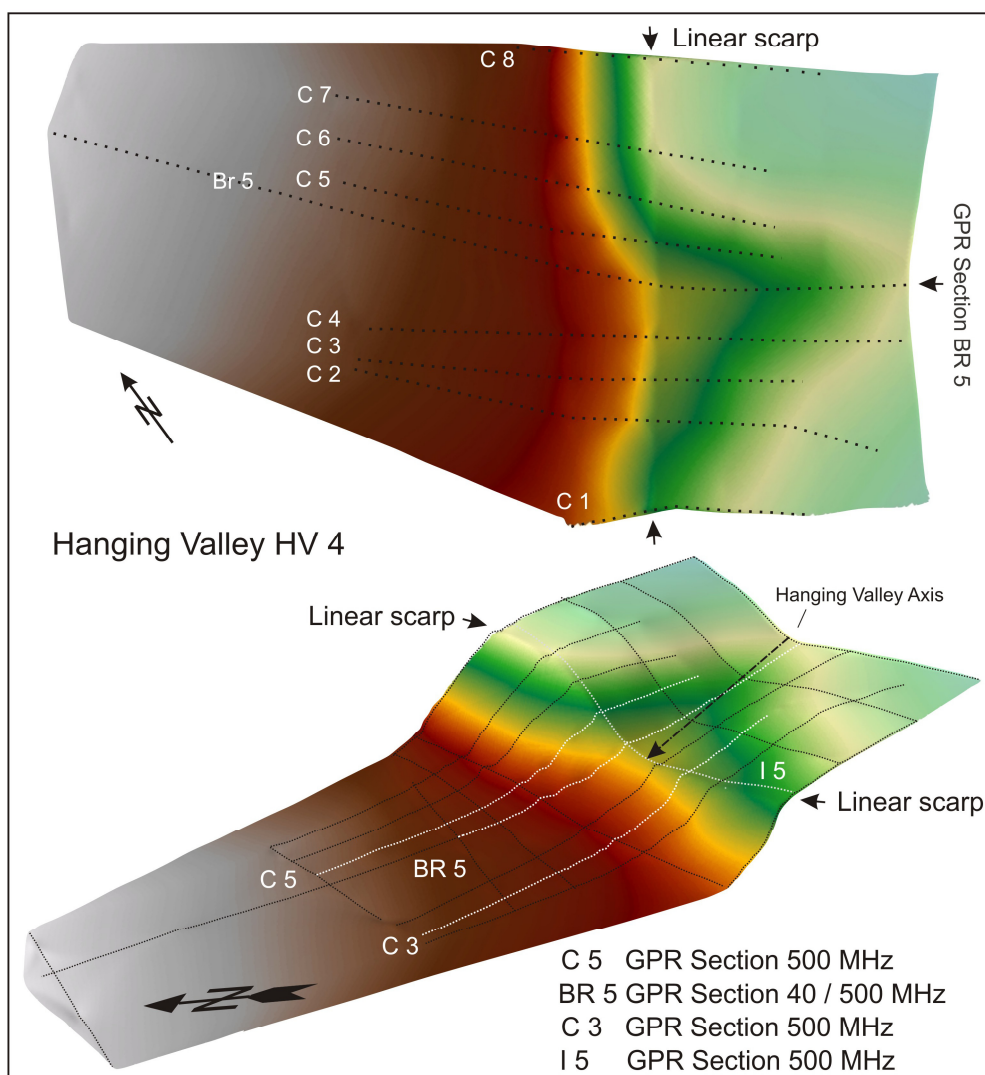


Fig. 8. High-resolution DEM of the hanging valley HV 4 derived from precise leveling (see Fig. 7 for location). Data show a marked knickpoint of the thalweg in the axis of the valley, which is related to a linear NE-trending morphological scarp crossing both valley flanks. The topographic sections are shown in Fig. 9.

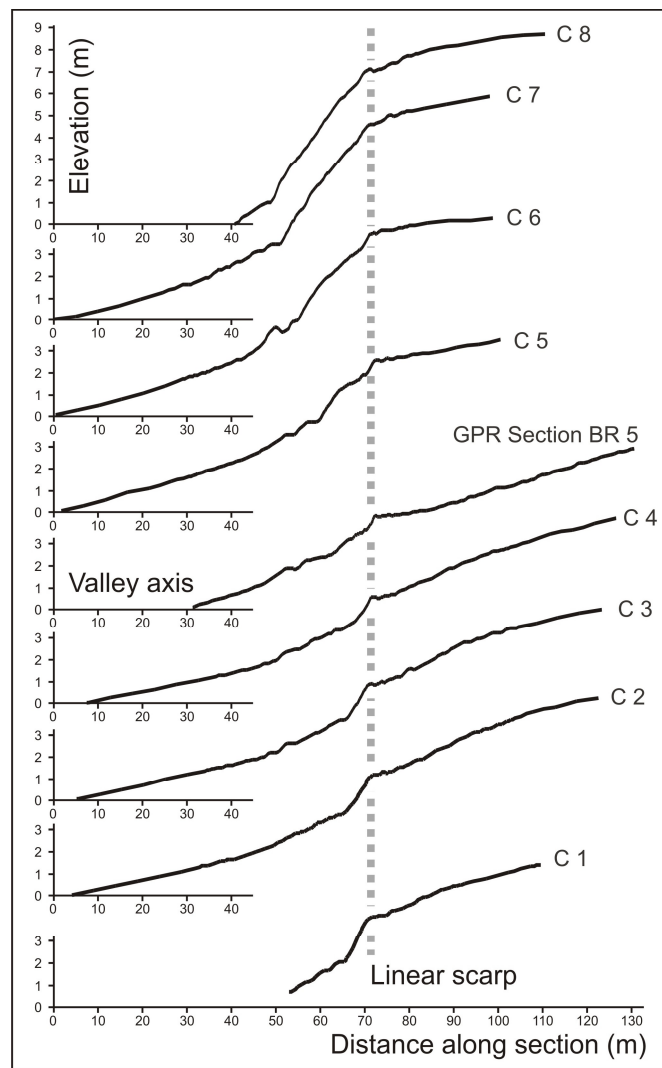


Fig. 9. Topographic sections in the hanging valley HV 4 derived from precise leveling (see Figs. 7 and 8 for location). All sections strike perpendicular to the general trend of the scarp. Data show pronounced c. 0.5 m high linear scarp transecting flanks and valley floor of HV 4.

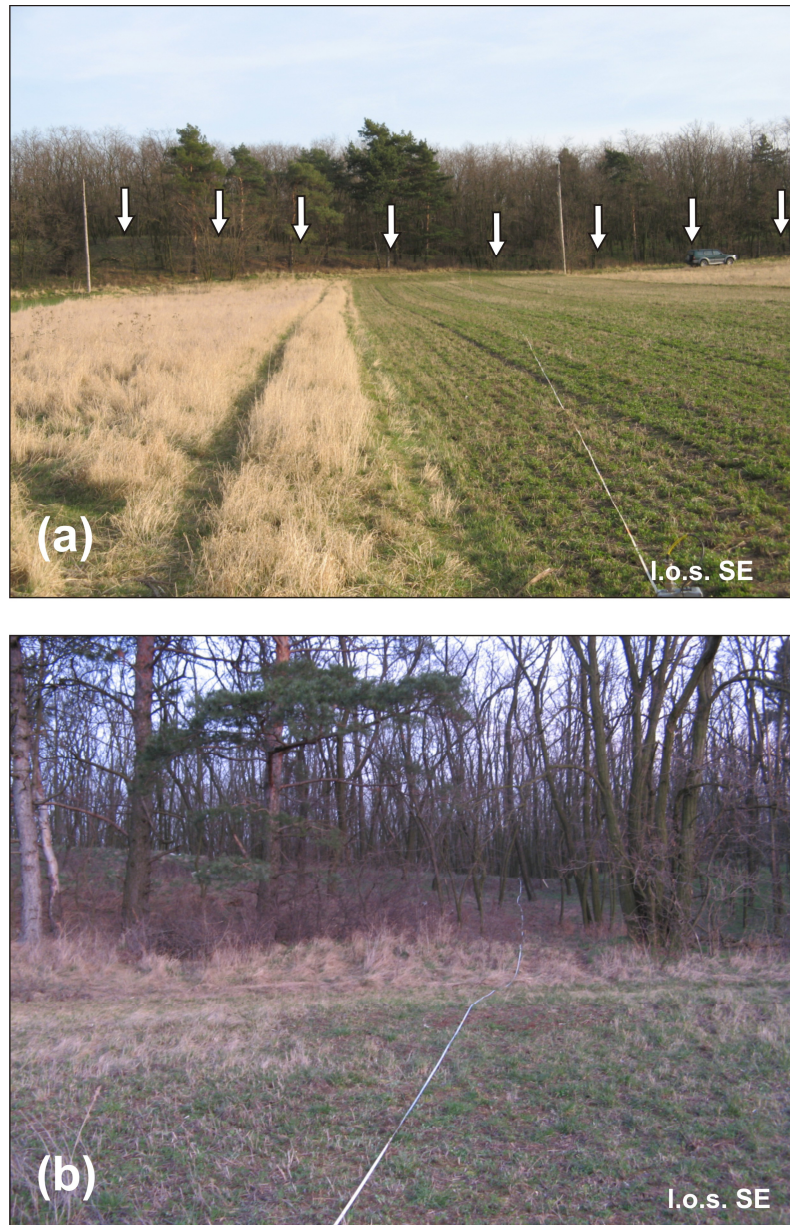


Fig. 10a. Field photographs of fault scarp 1 and the hanging valley HV 4 (see Fig. 5 for location). The trace of the Section BR-5 is indicated by a measuring tape. Note the sharply preserved scarp crossing the flank of the hanging valley (b). (l.o.s. – line of sight)

4.4.2. Georadar

GPR survey includes 4 crosslines perpendicular to the NE trending morphologic scarp of the Schlosshof Terrace of 350 to 700 m length, which are covered by measurements with both the 40 MHz and 500 MHz antenna (Fig. 7). In addition to these sections two 100 m long 500 MHz profiles were measured at the flanks of hanging valley HV4 (Fig. 8).

The 40 MHz sections are widely consistent in depicting the base of Pleistocene strata between 7 and 10 m depth below the surface on the elevated part of the terrace. This strong reflection corresponds to the lithological boundary between fine-grained Neogene sediments and Quaternary gravel, which overlie the Neogene strata (compare Fig. 3). GPR data show an angular unconformity between the two units (section BR 4, Fig. 11a). The base of Quaternary strata and the thickness of Quaternary sediments mapped from 40 MHz GPR profiles correlates well with borehole and outcrop data from gravel pits on the elevated part of the terrace (Fig. 7).

All GPR sections show that the reflector Base Quaternary disappears at the morphological scarp. Similar reflections are not found further to the NW (Fig. 11). There, borehole data indicate an increase of Quaternary sediment thickness with the Base Quaternary located at depths of up to 32 m, i.e., below the GPR penetration depth (Fig. 11c). We relate the truncation of the corresponding reflector to one or several faults with a cumulative normal displacement of some 35 m offsetting the base of Pleistocene strata from an elevation of about 165 m below the Schlosshof Terrace to an elevation of about 130 m at the margin of the Lasse Basin (Fig. 12). Section BR 6, which is located in the overlap region between the two sub-parallel scarps (Scarp 1 and 2, Fig. 7), shows that the base of Quaternary sediments is offset at both scarps. The offsets are associated with increasing thicknesses of Pleistocene gravel (Fig. 11c, 12). GPR results are corroborated by well data from a section 600 m NE of BR 6 indicating normal fault offsets of 5 m below Scarp 1 and 10 m below Scarp 2.

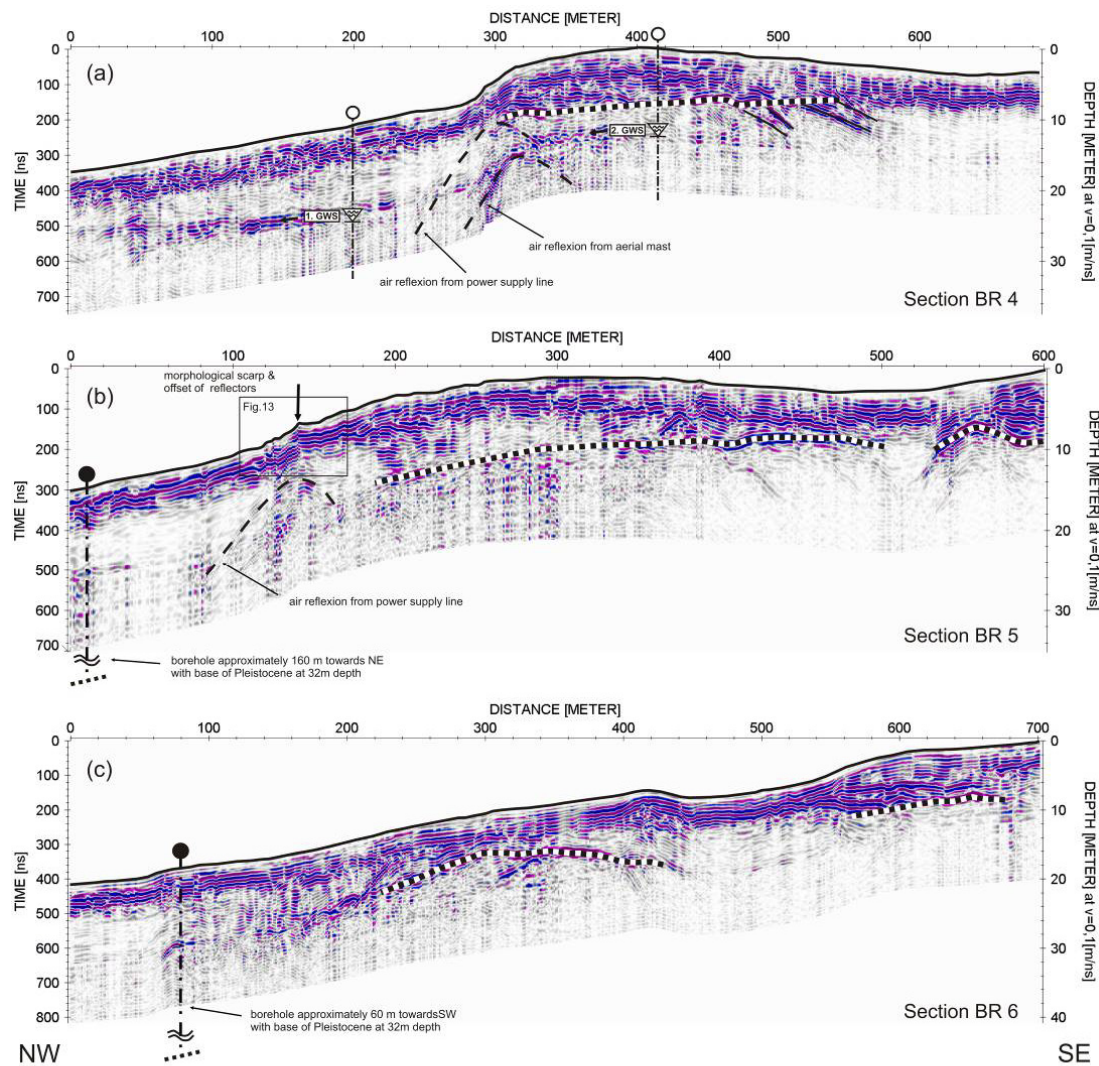


Fig. 11a. GPR 40 MHz Section BR 4 crossing scarp 1 (at about 300 m profile length) NW of the Schlosshof Terrace (see Fig. 7 for location). SE of the scarp: Pleistocene gravel (reflective upper unit) overlies Neogene sediments (transparent radar facies) with an angular unconformity. The Top Neogene (dashed line) is shown by a strong reflection, which terminates below the scarp. NW of the scarp the reflector appears to lie below GPR penetration depth of about 15 m. Reflections at about 12 m depth show the groundwater level as indicated by groundwater tubes. Boreholes SE of the scarp show a groundwater level at about 12 m depth.

Fig. 11b. GPR 40 MHz section BR 5 crossing scarp 1 (between 100 and 200 m distance; see Fig. 7 for location). The profile approximately follows the axis of hanging valley HV 4 (Fig. 8). The reflector Base Pleistocene (dashed line), which occurs at 7 to 10 m depth below the SE part of the section terminates at the scarp. Reflections within the Pleistocene underneath the scarp are offset (see GPR 500 MHz section BR 5 in Fig. 13 for detail).

Fig. 11c. GPR 40 MHz section BR 6 crossing scarp 1 (at 200 m) and 2 (at 550 m) NW of the Schlosshof Terrace (see Fig. 7 for location). The section is located in the overlap region between the two morphological scarps. The base of Pleistocene strata shows as a strong reflection between 7 to 10 m depth (dashed line), which is offset at both scarps. NW of scarp 1 this horizon is below the GPR penetration depth (i.e., below c. 12 m). Wells at this location show the Base Pleistocene at 32 m depth.

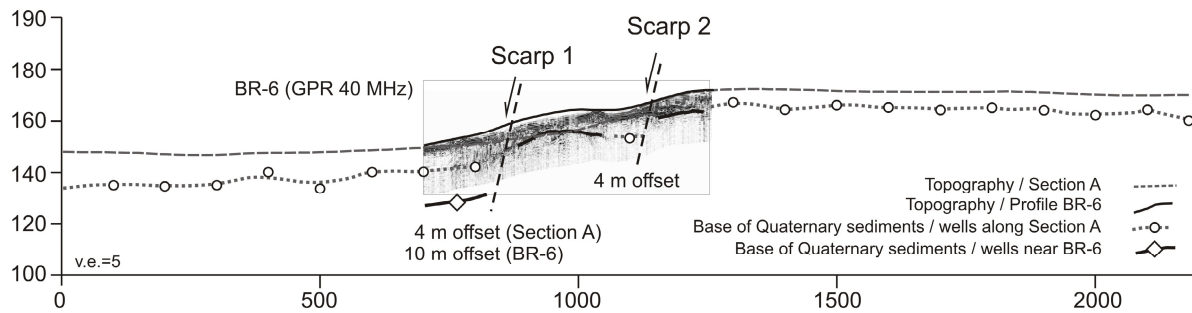


Fig. 12. GPR 40 MHz section BR-6 projected on a profile (Section A, see Fig. 7 for location) derived from wells about 600 m NE of BR-6. Projection direction is parallel to the trend of the scarps (see inset map). The base of Pleistocene strata is offset below both scarps as depicted by GPR and well data. Both vertical offsets are associated with an increase in Quaternary thickness indicating growth faults.

The results of the 500 MHz surveys, which were carried out for all GPR sections, are discussed for the profiles BR 5 and C 5 (Fig. 13, 14; see Fig. 8 for location). The 100 m long sections are located in the hanging valley HV4 spaced at a distance of about 20 m from each other. Both profiles depict several faults below Scarp 1. Faults are interpreted from marked discontinuities and/or sets of reflectors, which are vertically offset for about 20 to 50 cm at the interpreted faults. A surface breaking fault shown in both sections is exactly located at the position of the 50 cm high linear scarp crossing HV 4 (Fig. 8 to 10). GPR data indicate that reflectors are offset for about 30 to 40 cm at this fault. The offset inferred from GPR therefore approximates the height of the morphological scarp. In addition, both sections depict three other faults within a distance of about 10 m NW of the surface breaking fault. These faults can be traced up to a depth of about two meters being covered by about 1 – 2 m thick post-tectonic strata.

The position of faults mapped in the 500 MHz records matches faults imaged in the 40 MHz GPR section BR 5 (Fig. 13) and the truncation of the reflector Base of Quaternary recorded by the 40 MHz profiles.

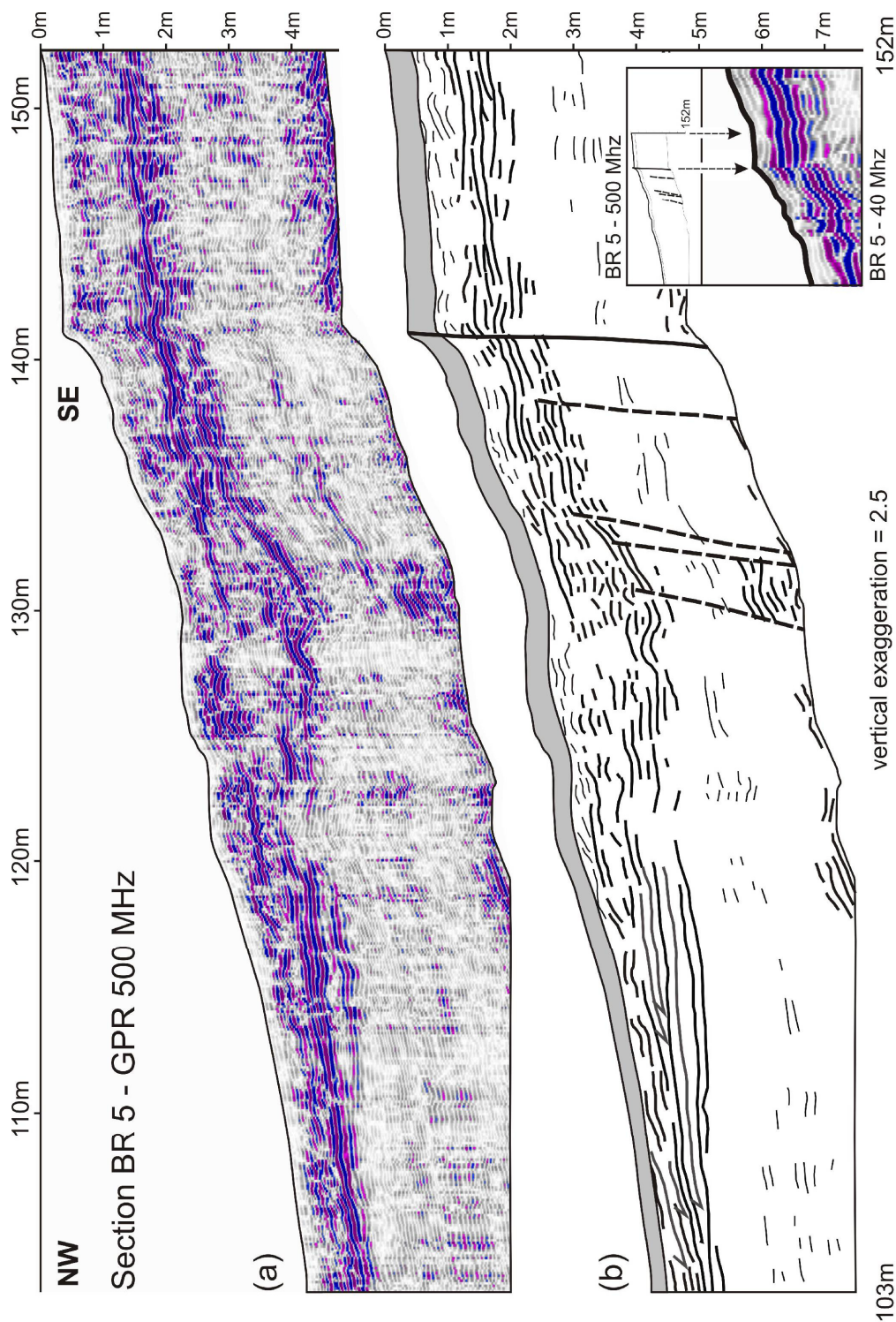


Fig. 13. GPR 500 MHz section BR 5 in hanging valley 4 (see Fig. 8 for location). The linear scarp crossing hanging valley 4 (Fig. 8) is situated at 142 m. Reflections below the scarp are offset suggesting a surface breaking fault with about 40 to 50 cm vertical displacement (compare enlarged inset). Discontinuous, warped and offset reflections further NW (between 130 and 140 m) indicate additional faults, which terminate upsection between 1 and 2 m depth. Faults apparently are covered by post-tectonic strata. Note downlaps of reflectors around 110 m. Grey hatching depicts the direct wave.

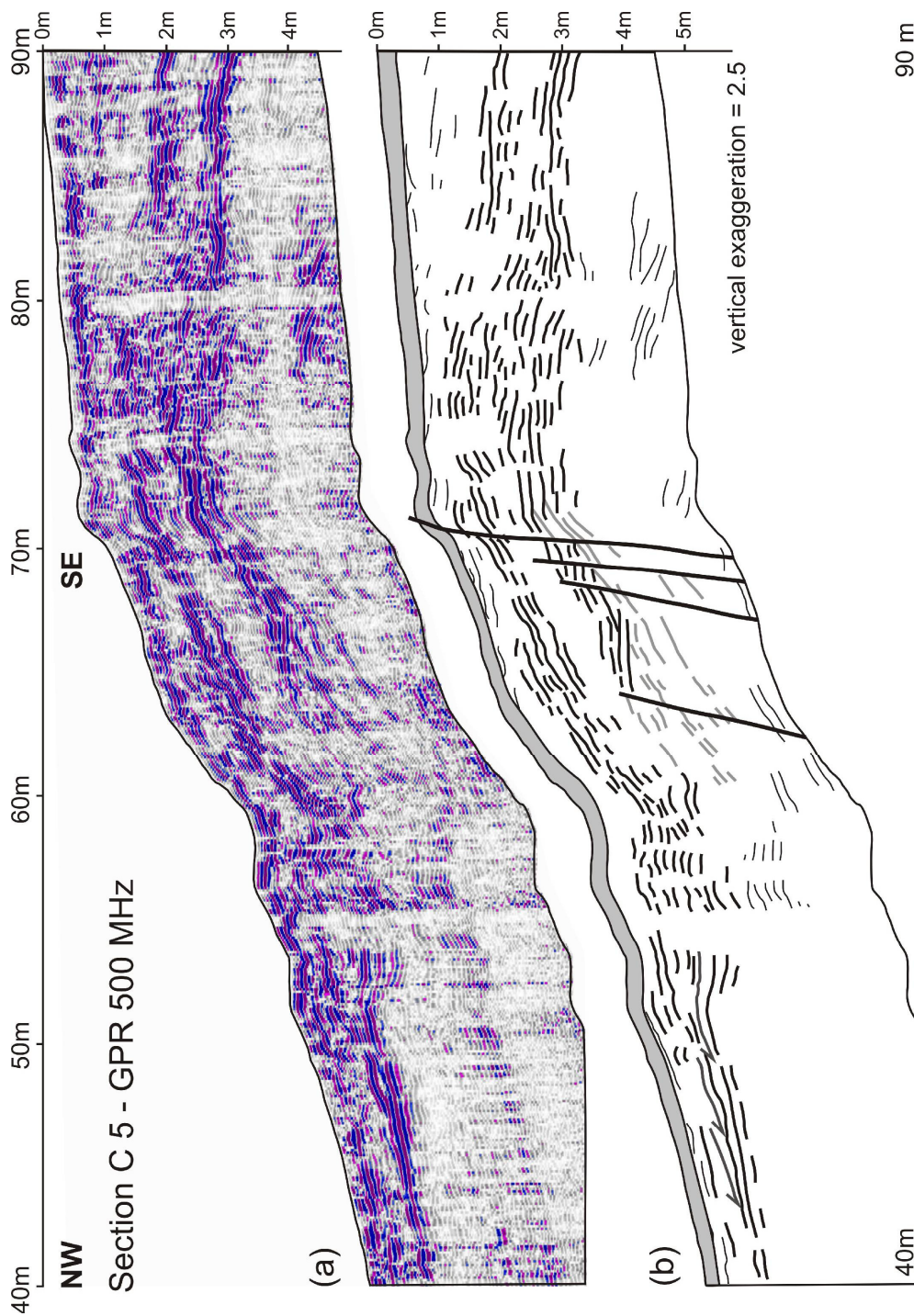


Fig. 14. GPR 500 MHz section C 5 in hanging valley 4 (see Fig. 8 for location). The lower band includes reflections discordantly covering dipping reflections (tagged in light grey in Fig. 14b). It is offset by faults at four locations. The upper band shows only a single major disturbance underneath the 0.5 m high linear scarp. To the NW it continues sub-parallel to the surface covering older faults. The inferred surface breaking fault at the scarp also offsets the lower set of reflections (compare with section BR-5, Fig. 16). Grey hatching depicts the direct wave.

4.5. Discussion

The following discussion focuses on an examination whether the Lassee segment may be regarded the source of the *Carnuntum* 4th century A.D. earthquake or not. For this purpose we shortly summarize evidence for active faulting along the segment and discuss its capability of producing significant earthquakes with respect to its overall dimension and the offsets observed at individual faults mapped below the scarps.

Geomorphologic, geological, borehole and high-resolution GPR data obtained during this study highlight the Lassee segment of the Vienna Basin fault system as an active fault, which is associated with at least two 15 to 20 m high fault scarps overlying splay faults of a negative flower structure. Quaternary fault activity is confirmed by the offset base of Pleistocene gravel and growth strata of Pleistocene age (Riss and younger, < 100 – 200 ky; Fig. 15). Growth strata thicken towards the center of the flower structure reaching a maximum thickness of some 120 m in the center of the Lassee Basin NW of the mapped scarps. Detailed GPR profiling show evidence for composite fault scarps with one scarp (scarp 1, Fig. 7) including faults terminating shortly below the surface. One of these faults is related to a scarp of some 50 cm height, which is superimposed on the composite scarp and shows only minor evidence of scarp degradation. The age of this feature, however, has not been determined yet.

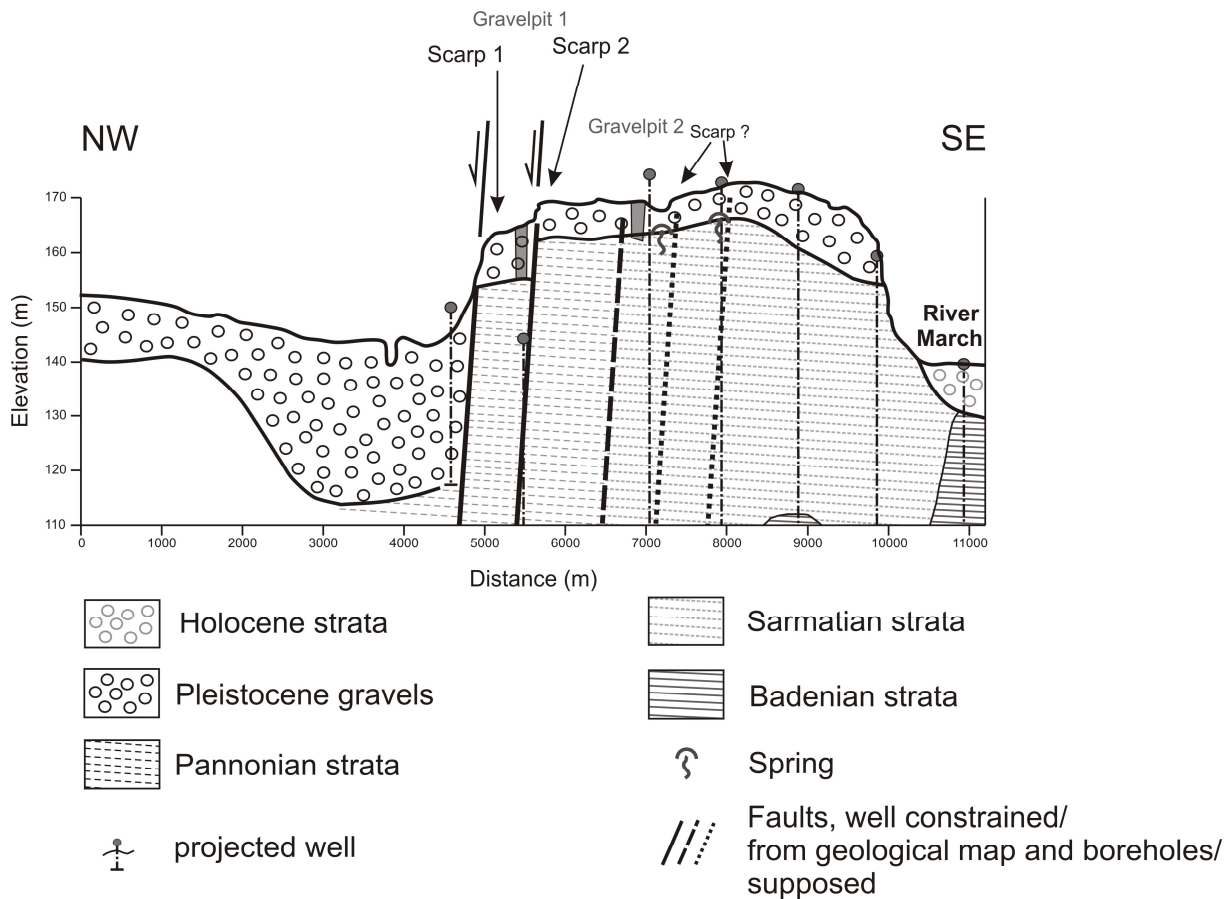


Fig. 15. Geological cross-section across the Lassesee Basin and the Schlosshof Terrace compilation from 40 MHz GPR data, tectonic geomorphology, wells and the geological map by Fuchs (1985). Two Quaternary growth faults are located at the parallel scarps at the NW margin of the Schlosshof Terrace bordering the Lassesee Basin. Geological data indicate additional faults with significant Miocene offset SE of the terrace boundary. Two of these faults coincide with possible fault controlled scarps in the elevated part of the plateau. The lithological section recorded in gravel pit 1 is shown in Fig. 3. See Fig. 3a for section location. Vertical exaggeration is approximately 70.

The minimum length of the Lassesee Fault Segment is estimated with 15 to 20 km assuming that segment boundaries of the strike-slip fault coincide with major oblique-normal faults, which branch off from the strike-slip fault SW and NE of the Lassesee Basin (see Hinsch et al., 2005b, for a discussion of fault segmentation; Hinsch & Decker, 2008). As the fault roots in a basal detachment of about 10 km depth formed by the Alpine-Carpathian floor thrust, a minimum total fault surface of $> 150 \text{ km}^2$ may be estimated, which may slip during a single seismic event. This surface is regarded large enough to produce events with $M > 6$ (Wells & Coppersmith, 1994; Vakov, 1996), which are comparable with the magnitude estimates for the *Carnuntum* 4th century, A.D. earthquake ($M_L = 6$ to 6.3 ± 1 ; Decker et al., 2006).

The vertical offsets of about 20 to 50 cm estimated from several faults cutting reflective bands in the 500 MHz GPR sections BR 5 and C 5 together with the dimension of the linear fault scarp of about 50 cm height enable a rough estimate of the intensity of events causing such surface displacement, provided that the offsets are related to coseismic surface rupture. This estimate uses the correlation between macroseismic intensity and surface displacement by Michetti et al. (2005; Fig. 16). Surface displacements of 20 to 50 cm, i.e. the vertical offsets observed at several faults at the composite Lassee scarp, correspond to earthquakes with intensity $I \sim 9 \pm 1$ MM (Modified Mercalli Scale). We stress that the intensity estimates are subject of large uncertainties due to both, uncertainties in the measured surface offset and the standard deviation of the used correlation. As the analyzed faults are parts of a sinistral strike slip fault system with a negative flower structure, we expect a strike-slip component of displacement, which can not be determined from the current dataset. However, estimates show that the formation of the surface breaking fault underlying the linear fault scarp in hanging valley HV4 may be related to a seismic event with an intensity comparable to the $I = 9 \pm 1$ earthquake of *Carnuntum* 4th century, A.D. (Decker et al., 2006), provided that the mapped fault offset formed during coseismic surface rupture.

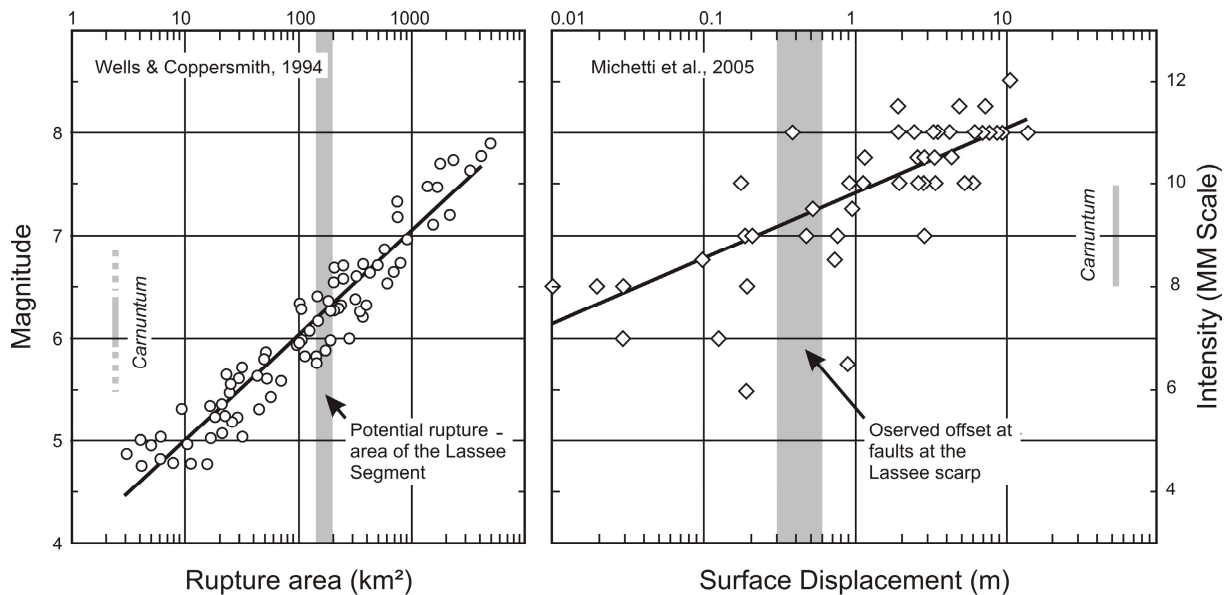


Fig. 16. Empirical relationship between rupture area and earthquake magnitude for strike-slip faults (a; after Wells & Coppersmith, 1994) and coseismic surface displacement and intensity (b; after Michetti et al. 2005). Grey hatching denotes the approximate fault area of the Lassee Segment (a) and the vertical displacement (20 to 50 cm) observed at faults imaged in 500 MHz GPR sections and the linear scarp

crossing hanging valley 4 (b). Both correlations indicate that the Lassee Segment is capable of producing earthquakes comparable to the size reconstructed for the *Carnuntum* 4th century earthquake.

Even though aseismic slip along the Vienna Basin Fault System and the Lassee segment in particular is not regarded as probable due to seismological and rheological considerations (see Hinsch & Decker, 2003, for detailed discussion) aseismic slip should not be fully excluded. Kelson & Baldwin (2001) and Stenner & Ueta (2000) stated from trench studies along active faults, that aseismic creep can produce features resembling those from coseismic surface ruptures. Sediment filled fissures, colluvial wedges resulting from scarp degradation and consistent upward termination of faults are diagnostic for coseismic ruptures. Upward fault terminations, however, may as well be produced by changes in the location of creeping strands through time. Such upward terminating faults are observed in 500 MHz sections BR 5 and C 5 whereas a colluvial wedge is indicated by stratal geometries in section BR 5. Reliable conclusions as to whether the revealed surface breaking faults depict coseismic surface ruptures or not can only be obtained by paleoseismologic trench studies.

4.6. Conclusions

Combined tectonic geomorphology and GPR studies reveal, independent from each other, a fault-controlled multiple event scarp at the NW border of the Upper Pleistocene Schlosshof Terrace indicating activity of the fault segment during the last 100 – 200 ky. The scarp is located some 14 km north of the Roman city of *Carnuntum*, which was damaged by a severe earthquake in the 4th century A.D. according to archeoseismological data (Kandler, 1989; Kandler et al., 2007). Tectonic morphology depicts segmentation of the fault with two sub-parallel scarps arranged in an en-echelon right stepping pattern. Both scarps are dissected by several hanging valleys. 40 MHz GPR sections reveal Pleistocene growth faults underneath both scarps offsetting the base of Quaternary gravels at the margin of the Lassee Quaternary basin, which includes up to 120 m thick Pleistocene growth strata in its centre. GPR interpretations are corroborated by Quaternary sediment thickness data

obtained from boreholes in the study area. Additional faults with probable Quaternary displacement transecting the center of the Schlosshof terrace are interpreted from geological data and the topography of the terrace (Fig. 15).

High resolution GPR measurements (500 MHz) show at least four faults offsetting Pleistocene strata proving continuous post-Pleistocene fault activity. Faults include a surface breaking fault related to a sharply defined linear scarp with some 50 cm height on the top of the multi-event scarp (scarp 1) at the NW boundary of the Schlosshof Terrace. Estimates of earthquake intensity using the vertical offset measured from 500 MHz GPR data and the height of the overlying fault scarp lead to an intensity of $I \sim 9 \pm 1$ (MM, Modified Mercalli Scale) for the scarp-forming event, provided that our data depicts coseismic surface rupture.

In sum, data support the interpretation that the Lassee Segment is a possible and probable source of the $I \sim 9 \pm 1$ (EMS-1998) *Carnuntum* 4th century, A.D. earthquake. Both the size of the fault surface of the Lassee segment and the documented offsets at individual splay faults indicate that the fault is capable of producing earthquakes with magnitudes / intensities comparable to the event documented by archeoseismology. It has further been argued that the most likely source for the *Carnuntum* earthquake should be located close to the damaged site (Decker et al., 2006). This reasoning is based on local intensity - distance relationships for the shallow earthquakes in the Vienna Basin, which show a rapid decrease of local intensity with distance from the epicenter. Accordingly, unreasonably high epicentral intensities must be assumed for seismic sources at distances of more than 10 km. The Lassee Fault, which passes the archaeological site at a distance of about 8 km, therefore appears as a likely seismic source for the 4th century event.

5. References

- ACORN, 2004. Seismic active discontinuities in the region "Eastern Alps-Western Carpathians-Bohemian Massif" based on geophysical data and digital seismic records of the seismic network "ACORN". W. A. Lenhardt (ed.), Federal Ministry for Education, Science and Culture, Vienna, 2004.
- Beidinger, A., Decker, K. & Roch, K.H., submitted. The Lassee segment of the Vienna Basin Fault System as a potential source of the earthquake of *Carnuntum* in the 4th century A.D. Submitted to: GSA Spec. Publ.
- Beidinger, A., Decker, K. & Roch, K.H., 2008. Combined geophysical, geomorphological and geological studies at the active Lasses Segment of the Vienna Basin Fault System. YORSGET-08, International Meeting of Young Researchers in Structural Geology and Tectonics, Oviedo, 1-3 July 2008, Programme & Extended Abstracts, 207-211.
- Bus, Z., Grenerczy, G., Tóth, L. & Mónus, P., in press. Active crustal deformation in two seismogenic zones of the Pannonian region - GPS versus seismological observations. Tectonophysics.
- Chwatal, W., Decker, K. & Roch, K.-H., 2005. Mapping of active capable faults by high-resolution geophysical methods: examples from the central Vienna Basin. Austrian Journal of Earth Sciences, 97, 52-59.
- Decker, K. & Burmester, G., 2008. Stress orientations and active fault kinematics of the Vienna Basin Fault System, Austria. 3rd Wold Stress Map Conference, Frontiers of Stress Research, Hemholtz Centre Potsdam, GFZ German Research Centre for Geosciences, Abstracts: p. 110.
- Decker, K., Gangl, G. & Kandler, M., 2006. The earthquake of Carnuntum in the 4th century AD - archaeological results, seismologic scenario and seismotectonic implications for the Vienna Basin Fault, Austria. Journal of Seismology, 10, 479-495.
- Decker, K., Peresson, H., & Hinsch, R., 2005. Active tectonics and Quaternary basin formation along the Vienna Basin Transform fault. Quaternary Sci. Rev., 24, 307-322.
- Decker, K. & Peresson, H., 1998. Miocene to present-day tectonics of the Vienna Basin transform fault: Links between the Alps and the Carpathians, Abstr. Carpathian-Balkan Geological Association XVI Congress, August 30th to September 2nd: pp. 33-36, Vienna (Geol. B. A.).
- Decker, K., 1996. Miocene tectonics at the Alpine-Carpathian junction and the evolution of the Vienna Basin. Mitt. Ges. Geol. Bergbaustud., 41: 33-44.
- Fendek, M. & Fendekova, M., 2005. Transboundary flow modeling: the Zohor depression of Austria and the Slovak Republic. Groundwater, 43/5: 717-721.

Fink, J., 1973. Zur Morphogenese des Wiener Raumes. Z. Geomorph. N.G., Suppl. 17: 91-117 (Berlin-Stuttgart).

Fink, J., 1955. Das Marchfeld. Verhandlungen der Geologische Bundesanstalt, Spec. Vol. D: 88-116.

Fodor, L., 1995. From transpression to transtension: Oligocene-Miocene structural evolution of the Vienna Basin and the East Alpine-Western Carpathian junction. Tectonophysics 242: 151-182.

Fuchs, W., 1985. Geological map of Austria, No. 61-62, Hainburg an der Donau – Pressburg 1 : 50.000, Vienna (Geologische Bundesanstalt)

Fuchs, W. & Grill, R., 1984. Geologische Karte von Wien und Umgebung 1 : 200.000. Wien (Geol. B.-A.)

Glodny J., Ring U., Kühn A. (2008) Coeval high-pressure metamorphism, thrusting, strike-slip and extensional shearing in the Tauern Window, Eastern Alps. Tectonics 27, TC4004, doi:10.1029/2007TC002193

Gradstein, F. & Ogg., J., 2004. Geologic Time Scale 2004 - why, how, and where next! Lethaia, 37: 175-181.

Grenerczy, G., 2002. Tectonic processes in the Eurasian-African plate boundary zone revealed by space geodesy. In: S. Stein and J.T. Freymueller (Editors), Plate Boundary Zones. AGU Monograph. American Geophysical Union, pp. 67-86.

Grenerczy, G., Kenyeres, A. & Fejes, I. 2000: Present crustal movement and strain distribution in Central Europe inferred from GPS measurements. J. Geophys. Research 105 B9: 21.835-21.846.

Grünthal, G., Mayer-Rosa, D. & Lenhardt, W., 1998. Abschätzung der Erdbebengefährdung für die D-A-CH-Staaten – Deutschland, Österreich, Schweiz. Bautechnik, 10: 19-33.

Gutdeutsch, R & Aric, K. 1988: Seismicity and neotectonics of the East Alpine-Carpathian and Pannonian area. AAPG Memoir 45: 183-194.

Harzhauser, M. & Piller, W., 2004. The Early Sarmatian – hidden seasaw changes. Cour. Forschungsinst. Senckenberg, 246: 89-112.

Häusler, H., Leber, D., Peresson, H. & Hamilton, W., 2002. A New Exploration Approach in a Mature Basin: Integration of 3-D Seismic, Remote-sensing, and Microtectonic Data, Southern Vienna Basin, Austria. In: D. Schumacher and L. A. LeSchack (eds.), Surface Exploration Case Histories: Applications of Geochemistry, Magnetism, and Remote Sensing, AAPG Studies in Geology, 48: 433-451.

Hinsch, R. & Decker, K., 2008. Reassessing seismic-slip values and potential seismogenic fault areas in the Vienna Basin: implications for seismic potential. *Journal of Alpine Geology*, 49: 41.

Hinsch, R., Decker, K., & Pereson, H., 2005a. 3-D seismic interpretation and structural modeling in the Vienna Basin: implications for Miocene to recent kinematics. *Austrian Journal of Earth Sciences*, 97, 38-50.

Hinsch, R., Decker, K. & Wagreeich, M., 2005b, 3-D Mapping of segmented active faults in the southern Vienna Basin, *Quaternary Sci. Rev.*, 24, 321-336.

Hinsch, R. & Decker, K., 2003. Do seismic slip deficits indicate an underestimated earthquake potential along the Vienna Basin Transform Fault System? *Terra Nova* 15 (5), 343-349.

Hölzel, M., Decker, K., Zámolyi, A., Strauss, P. & Wagreeich, M., in press. Lower Miocene structural evolution of the central Vienna Basin (Austria). *Basin Research*.

Hölzel, M., Wagreeich, M., Faber, R., & Strauss, P., 2008. Regional subsidence analysis in the Vienna Basin (Austria). *Austrian Journal of Earth Sciences*, 101: 88-98.

Humer, F. & Maschek, D., 2007. Eine Erdbebenzerstörung des 4. Jahrhunderts n. Chr. Im sogenannten Peristylhaus der Zivilstadt Carnuntum. *Aarchäologie Österreichs*, 18/2: 45 – 55.

Kandler, M., Decker, K. & Gangl, G., 2007. Archäologische Befunde von Erdbebenschäden im Raum von Carnuntum und ihre seismotektonische Interpretation. In: G. H. Waldherr, A. Smolka (eds.), *Antike Erdbeben im alpinen und zirkualpinen Raum*, *Geographica Historica*, 24, 11-132, Stuttgart.

Kandler, M., 1989, Eine Erdbebenkatastrophe in Carnuntum? *Acta Archaeologica Academia Scientarum Hungarica* 41, 313-336, Budapest (Akademia Kiado)

Kelson, K.I., & Baldwin, J.N., 2001. Can paleoseismologic techniques differentiate between aseismic creep and coseismic surface rupture? *Seismological Research Letters* 72, 263 (abstract)

Kováč, M., Barath, I., Harzhauser, M., Hlavaty, I., Hudackova, N., 2004. Miocene depositional systems and sequence stratigraphy of the Vienna Basin. *Courier Forschungs-Institut Senckenberg*, 246: 187-212.

Kröll, A. & Wessely, G., 1993. Wiener Becken und angrenzende Gebiete - Strukturkarte-Basis der tertiären Beckenfüllung. *Geologische Themenkarte der Republik Österreich* 1:200.000.

Kullmann, E., 1966. Le rôle des mouvements néotectoniques dans la création de réservoirs d'eaux souterraines dans la partie nord-est du Bassin de Vienne. IAHS, Redbooks: 120, pp. 392-400.

Küpper H 1952. Neue Daten zur jüngsten Geschichte des Wiener Beckens. Mitt. Geograph. Ges.: 94/1-4: 10-30.

Lenhardt, W., Freudenthaler, C., Lipitsch, R & Figweil, E., 2007. Focal-depth distributions in the Austrian Eastern Alps based on macroseismic data. Austrian Journal of Earth Sciences, 100: 66-79.

Linzer, H.-G., Decker, K., Peresson, H., Dell'Mour, R., & Frisch, W. 2002. Balancing lateral orogenic float of the Eastern Alps. Tectonophysics, 354 (3-4): 211-237.

Linzer, H.-G., Moser, F., Nemes, F., Ratschbacher, L. & Sperner, B., 1997. Build-up and dismembering of a classical fold-thrust belt: from non-cylindrical stacking to lateral extrusion in the eastern Northern Calcareous Alps Tectonophysics 272: 97-142.

Mandl, G., 1988. Mechanics of tectonic faulting. Models and basic concepts. Developments in Structural Geology, 1: 407 pp. (Elsevier).

Marko, F., Fodor, L. & Kovác, M., 1991. Miocene strike slip faulting and block rotation in Brezovské Karpaty Mts. (Western Carpathians). Mineralia slovaca, 23: 189 200.

Michetti, A., Audermard, F. & Marco, S., 2005. Future trends in paleoseismology: Integrated study of the seismic landscape as a vital tool in seismic hazard analyses. Tectonophysics, 408: 3-21.

Naylor, M.A., Mandl, G. & Sijpesteijn, C.H.K., 1986. Fault geometries in basement-induced wrench faulting under different initial stress states. Journal of Structural Geology, 8(7): 737-752.

Peresson, H. & Decker, K., 1997. Far-field effects of Late Miocene subduction in the Eastern Carpatians: E-W compression and inversion of structures in the Alpine-Carpatian-Pannonian region, Tectonics, 16 (1): 38-56.

Piller, W., Egger, H., Gross, M., Harzhauser, M., Hubmann, B., van Husen, D., Krenmayr, H.-G., Krystyn, L., Lein, R., Mandl, G., Rögl, F., Roetzel, R., Rupp, C., Schnabel, W., Schönlaub, H. P., Summesberger, H. & Wagreich, M., 2004. Die Stratigraphische Tabelle von Österreich 2004 (Sedimentäre Schichtfolgen). Ber. Inst. Erdwiss., Graz (Karl-Franzens Universität), 9: 329-330.

Ratschbacher, L., Merle, O., Davy, P. & Cobbold, P., 1991a. Lateral extrusion in the eastern Alps, part I: boundary conditions and experiments scaled for gravity. Tectonics, 10(2): 245-256.

Ratschbacher, L., Frisch, W. & Linzer, H.-G., 1991b. Lateral extrusion in the eastern Alps, part II: structural analysis. *Tectonics*, 10 (2): 257-271.

Reinecker, J. & Lenhardt, W.A. 1999. Present-day stress field and deformation in eastern Austria. *Int. Journ. Earth Sciences* 88: 532-530.

Richard, P.D., Naylor, M.A., Koopman, A., 1995. Experimental models of strike-slip tectonics. *Petroleum Geoscience* 1, 71–88.

Riedel, W., 1929. Zur Mechanik geologischer Brucherscheinungen. *Centralblatt für Mineralogie, Abt. B*, 1929: 354-368.

Rögl, F., Zapfe, H., Bernor, R.L., Brzobohaty, L., Daxner Höck, G., Draxler, I., Fejfar, O., Gaudant, J., Herrmann, P., Rabeder, G., Schultz, O. and Zetter, R., 1993. Die Primatenfundstelle Götzendorf an der Leitha (Obermiozän des Wiener Beckens, Niederösterreich). *Jb. Geol. B. A.*, 136/2: 503-526.

Rögl, F., 1996. Stratigraphic correlation of the Paratethys (Oligocene and Miocene). *Mitt. Ges. Geol. Bergbaustud. Österr.*, 41: 65-73.

Royden, L.H., 1985. The Vienna Basin: A thin-skinned pull-apart basin. In: Biddle, K.T. and Christie-Blick, N. (eds.). *Strike slip deformation, basin formation and sedimentation*. *SEPM Spec.Publ.*, 37: 319-338.

Royden, L., 1988. Late Cenozoic tectonics of the Pannonian basin system. In: Royden, L.H. and Horváth, F. (eds.). *Am. Assoc. Petrol.Geol., Mem.*, 45: 27-48.

Salcher, B., Meurers, B., Decker, K. & Wagneich, M., submitted. First order derivatives from conventional Bouguer gravity data: Detection of very shallow structures in an active pull apart (Vienna Basin). Submitted to: *Basin Research*.

Sauer, R., Seifert, P. and Wessely, G., 1992. Guidbook to excursions in the Vienna Basin and the adjacent Alpine-Carpathian thrustbelt in Austria. *Mitt.Geol.Ges.*, 85: 1-264.

Schlische, R.W., Withjack, M.O., and Eisenstadt, G., 2002, An experimental study of the secondary deformation produced by oblique-slip normal faulting: *AAPG Bulletin*, 86: 885-906.

Stenner, H.D., Ueta, K., 2000. Looking for evidence of large surface rupturing events on the rapidly creeping southern Calaveras fault, California in Active Fault research for the new millennium. In: Okumura, K., Takada, K., Goto, H. (Eds.), *Proceedings of the Hokudan International Symposium and School on the Active Faulting*. Hokudan Co. Ltd., Hokudan, Hyogo, Japan, pp. 479–486.

Strauss, P., Harzhauser, M., Hinsch, R. & Wagneich, M., 2006. Sequence stratigraphy in a classic pull-apart basin (Neogene, Vienna Basin). A 3D seismic based integrated approach. *Geologica Carpatica*, 57/3: 185-197.

Urbanek, C., Frank, W., Grasemann, B. & Decker, K., 2002. Eoalpine versus Tertiary deformation: Dating of heterogeneously partitioned strain (Tauern Window, Austria). Abstr. Pangeo Austria I: 183-184 (Univ. Salzburg).

Thenius, E. 1956. Neue Wirbeltierfunde aus dem Ältestpleistozän von Niederösterreich. Zur Stratifizierung der Donauterrassen. Jb. Geol. B.-A., 99: 259-271.

Vakov, A. V., 1996. Relationship between earthquake magnitude, source geometry and slip mechanism, Tectonophysics, 261, 97—113.

Van Husen, D., 2000. Geological processes during the Quaternary. Mitt. Österr. Geol. Ges. 92: 135-156.

Wagreich, M. & Schmid, H.P., 2002. Backstripping dip-slip fault histories: apparent slip rates for the Miocene of the Vienna Basin. Terra Nova, 14/3: 163 – 168.

Wells, D.L. & Coppersmith, K.J., 1994. New Empirical Relationships among Magnitude, Rupture Length, Rupture Width, Rupture Area, and Surface Displacement, Bulletin of the Seismological Society of America 84, 974-1002.

Wessely, G., 1988. Structure and development of the Vienna basin in Austria. In: Royden, L.H. and Horváth, F. (eds.). Am. Assoc. Petrol. Geol., Mem., 45: 333-346.

ZAMG [Zentralanstalt für Meteorologie und Geodynamik] 2008. Catalogue of felt earthquakes in Austria 1201-2007. Computer file, Vienna (ZAMG).

Appendix

I. Abstract

The sinistral active Vienna Basin Fault System (VBFS) extends from the Eastern Alps through the Vienna Basin into the West Carpathians. It consists of several strike slip segments, which differ both in their kinematic and seismologic properties. Among these, the Lassee segment 30 km east of Vienna is of particular interest for seismic hazard assessment as it shows a marked seismic slip deficit. The segment is located about 8 km from the Roman city of *Carnuntum*, for which archaeological data indicate a destructive earthquake in the 4th century AD (local intensity about 9 EMS-1998).

Seismic mapping of a grid of industrial 2D seismic lines crossing the Quaternary Lassee basin and the adjacent Pleistocene terraces about 30 km E of Vienna (Lassee Segment) depicts a negative flower structure, which developed during the Middle and Upper Miocene. The flower structure consists of several splay faults, which are regarded as Riedel shears and mostly merge at the interface between the pre-Neogene basement and the Miocene basin fill. However, the major branch line which marks the top of the principle displacement zone is situated at depths of about 3500 m to 5500 m and is not controlled by this interface. Growth strata show that major fault activity within the flower occurred between the Upper Sarmatian and Upper Pannonian. The maximum vertical displacement of 1150 m occurs along an 800 m wide fault zone at the SE border of the flower. The heterogeneous distribution of vertical offset results in an asymmetric shape of the flower structure with horizons dipping towards SE. Pleistocene basin analyses and tectonic geomorphology prove continued faulting during the Quaternary by reactivation of Miocene faults. This is depicted by the asymmetric shaped Pleistocene Lassee basin overlying the flower structure, tilting of surface topography and fault controlled scarps.

The basin with up to 120 m Quaternary sediments is confined by elevated Middle Pleistocene terraces to both sides. The terraces show en-echelon, right stepping morphological scarps, which coincide with faults mapped in seismic.

Mapping the PDZ of the Vienna Basin fault system by using additional 2D seismic data in the NE and SW continuation of the Lassee segment reveals several segments along the active strike-slip fault, which differ by the orientation of the PDZ. NE- and NNE-striking segments with releasing bend geometries are associated with Quaternary basins. These segments are connected by ENE-striking segments orientated parallel to the displacement vector. Among the releasing bends, the Lassee segment is subject to increased extension due to the high angle (35°) between the general slip vector and the orientation of the segment. Resulting extension seems to be accommodated by both, the negative flower structure and normal faults (Markgrafneusiedl fault and its antithetic faults), which branch off from the PDZ south of the Lassee releasing bend.

For the reconstruction of the youngest faulting history of the Lassee segment GPR studies and additional geomorphologic studies at the NW scarp of the Schlosshof terrace were obtained. The about 20m high morphological scarp coincides with the fault zone at the SE boundary of the flower structure. There, high-resolution GPR (40 MHz, 500 MHz) mapped at least four distinct surface-breaking faults along this scarp including three faults, which are covered by about 2 m of post-tectonic strata. The youngest fault offsets these strata and coincides with a 0.5 m high scarp, which seems to be the product of a surface breaking earthquake. Data indicate that the Lassee Segment may well be regarded the source of the 4th century earthquake. The interpretation is in line with local attenuation relations indicating a source close to the damaged site, observed fault dimensions and the fault offsets recorded by GPR and morphology.

II. Abstract (German)

Das aktive sinistrale Wiener Becken Störungssystem erstreckt sich von den Ostalpen entlang des Wiener Beckens bis in die westlichen Karpaten. Es ist durch zahlreiche Blattverschiebungssegmente gekennzeichnet, die unterschiedliche kinematische und seismotektonische Charakteristika aufweisen. Unter diesen zeigt das Lasseer Segment ein deutliches seismisches Versatzdefizit auf. Es ist dadurch für zukünftige Erdbebenrisikoanalysen von besonderem Interesse. Das Segment liegt ca. 30 km östlich von Wien und ca. 8 km westlich von der historischen römischen Siedlung *Carnuntum*. Archäologische Untersuchungen zeigen eine Zerstörung dieser Siedlung im 4. Jhdt. n. Chr. durch ein Erdbeben mit einer Intensität I ~ 9 EMS-98.

Die Kartierung des Segments mit Hilfe von 2D Seismiklinien, die von OMV Austria zur Verfügung gestellt wurden, zeigt eine negative Blumenstruktur, die während dem Mittleren und Oberen Miozän aktiv war. Die Blumenstruktur weist zahlreiche, von der Grenzfläche zwischen dem Präneogenem Untergrund des Wiener Beckens und der Miozänen Beckenfüllung abzweigende Störungen auf, welche als Riedel-Störungen interpretiert werden. Diese Abzweigungen in unmittelbarer Nähe zum Präneogenen Untergrund sind auf den rheologischen Kontrast zwischen diesem und der Miozänen Beckenfüllung zurückzuführen. Im Gegensatz dazu ist die Hauptabzweigungslinie, welche alle nordwestlichen und südöstlichen abzweigenden Störungsstränge verbindet, nicht an diese rheologische Grenzfläche gebunden.

Die Bestimmung von "growth strata" zeigt signifikante Störungsaktivität vom Oberen Sarmat bis ins Obere Pannon, wobei die Störungszone, welche die Blumenstruktur nach Südosten abgrenzt, die größten vertikalen Versatzbeträge aufweist (1150 m). Diese heterogene Verteilung des vertikalen Versatzes resultiert in einer asymmetrischen Form der Blumenstruktur mit nach SE gegen die Störungszone einfallenden Schichten. Analysen von quartären Sedimentbecken und tektonischer Geomorphologie zeigen eine Quartäre Reaktivierung der Miozänen Störungen. Dies wird von der Asymmetrie der die Blumenstruktur überlagernden Quartären Lasseer

Beckens, dem Einfallen der Oberflächentopographie gegen die Störungszone am südöstlichen Rand der Blumenstruktur und von störungskontrollierten morphologischen Geländestufen (fault scarps) abgeleitet.

Das Quartäre Lasee Becken, das bis zu 120 m Quartäre Sedimente enthält, ist gegen NW und SE durch NE-streichende segmentierte, in rechtstretenden en-echelon-Mustern angeordnete Geländestufen gegen höherliegende Pleistozäne Terrassen abgegrenzt.

Diese morphologischen Stufen überlagern Störungen, die innerhalb der Blumenstruktur signifikanten vertikalen Versatz aufweisen. Sie werden daher als fault scarps interpretiert, die von en-echelon angeordneten, rechtstretenden, sinistralen Schrägabschiebungen kontrolliert werden.

Die Kartierung der Hauptabzweigungslinie unter Verwendung zusätzlicher 2D Seismiklinien in der nordöstlichen und südwestlichen Fortsetzung des Lasee Segments, zeigt zahlreiche aktive Störungssegmente. NE- und NNE-streichende Segmente, die mit darüberliegenden Quartären Becken assoziiert sind, werden als releasing bends interpretiert. Diese sind durch ENE-streichende Segmente, die parallel zum Versatzvektor orientiert sind, verbunden. Aufgrund des erhöhten Winkels zum Versatzvektor, ist das NNE-streichende Lasee Segment einer erhöhten Extension ausgesetzt. Dieser erhöhte Extensionsbetrag wird mit großer Wahrscheinlichkeit durch die Abschiebungen des Markgrafneusiedl- und Aderklaa Bruchs im WNW akkommodiert. Diese Störungen werden ebenfalls von Quartären Becken (Obersiebenbrunn Becken, Aderklaa Becken) überlagert.

Zur Rekonstruktion der jüngsten Störungsgeschichte entlang des Lasee Segments wurden Georadarstudien sowie zusätzliche tektonische Geomorphologiestudien an einem Scarp am NW-Rand der Schlosshof Terrasse durchgeführt. Dieser ca. 20 m hohe Scarp liegt über einer Störungszone am südöstlichen Rand der Blumenstruktur. Die Ergebnisse der Georadarstudien (40MHz und 500MHz) zeigen mindestens vier Störungen, die bis an die Oberfläche kartiert werden können. Eine der Störungen fällt mit einer ca. 0.5 m hohen Stufe zusammen, die mit einem jüngeren Erdbebenereignis in Zusammenhang gebracht werden könnte. Die Ergebnisse zeigen, dass das Lasee Segment eine mögliche Quelle für das Erdbeben von *Carnuntum* im 4. Jhdt. n. Chr. darstellt. Diese Interpretation ist

mit lokalen Abschwächungsfunktionen, die eine nahe gelegene Quelle für das Erdbeben erfordern, den Größenordnungen der beobachteten Versätze aus der Georadarstudie, der Störungsgröße des Lasseer Segments und tektonisch-geomorphologischen Daten im Einklang.

Curriculum vitae

Name		Andreas Beidinger
Geburtsdatum, -ort		18. 06. 1981, Oberpullendorf
Staatsbürgerschaft		Österreich
Familienstand		ledig
Anschrift		Hauptstraße 47, A-7302 Nikitsch Tel.: 00436649431667 Email: andreas.beidinger@gmx.net
Schulbildung	1987-1991	Volksschule Nikitsch
	1991-1995	BRG Oberpullendorf
	1995-2000	HTBLA Eisenstadt, Ausbildungszweig Flugtechnik, Matura mit ausgezeichnetem Erfolg
Hochschulbildung	10/2001-02/2002	FH Joanneum-Graz, Studiengang Luftfahrt/Aviation
	10/2002-03/2003	Außerordentlich Studierender an der Universität Wien
	03/2003-10/2006	Universität Wien, Bakkalaureatsstudium Erdwissenschaften, Abschluss mit ausgezeichnetem Erfolg
	Seit 10/2006	Universität Wien, Magisterstudium Erdwissenschaften
	02/2008-08/2008	Auslandsaufenthalt im Rahmen von ERASMUS an der Universidad de Oviedo, Spanien
Präsenzdienst	10/2000-05/2001	Langenlebarn und Wr. Neustadt
Berufserfahrung	01/2001-10/2002	Dialog Direkt (Direktwerbung), mit Einsatz im Ausland und Tätigkeit als Teamleiter
	07/2005-12/2007	NUA-Umweltanalytik GmbH, Probenehmer (geringfügig beschäftigt)

Seit 08/2008

Universität Wien, Projektmitarbeiter am
Department für Geodynamik und
Sedimentologie

Besondere Kenntnisse

Burgenländisch Kroatisch
(Muttersprache)
Englisch (in Wort und Schrift)
Spanisch (Niveau B1)
Führerschein A, B, C, F, G

Absolvierte Konferenzen

*EGU, General Assembly 2007, 15.-20. April 2007, Vienna Austria;
Posterpräsentation:*

Beidinger, A., Decker, K., Roch, K.-H., Grasemann, B. (2007). 3D Geometry of the active Lassee flower structure (Vienna Basin Fault System): data from integrated geophysical, geomorphological and geological mapping. Geophysical Research Abstracts: 9.

*EGU, General Assembly 2008, 13.-18. April 2008, Vienna, Austria;
Posterpräsentation:*

Beidinger, A., Decker, K. (2008). Fault patterns and fault-controlled topography at a releasing bend of the Vienna Basin Fault System. Geophysical Research Abstracts: 10.

*SSA Annual Meeting 2008, 16.-18. April 2008, Santa Fe, New Mexico, USA;
Kurzvortrag:*

Beidinger, A., Decker, K., Roch, K.-H. (2008). The Vienna Basin Fault System as a potential source of the earthquake of *Carnuntum* in the 4th century A. D.. Seismological Research Letters: 79(2).

International Meeting of Young Researchers in Structural Geology and Tectonics (YORSGET), 01.-03. Juli 2008, Oviedo, Spain; Kurzvortrag:

Beidinger, A., Decker, K. & Roch, K.H., 2008. Combined geophysical, geomorphological and geological studies at the active Lassee Segment of the Vienna Basin Fault System. YORSGET-08, International Meeting of Young Researchers in Structural Geology and Tectonics, Oviedo, 1-3 July 2008, Programme & Extended Abstracts, 207-211.